SPATIAL DEPENDENCE AND AGGREGATION IN WEATHER RISK HEDGING: A LÉVY SUBORDINATED HIERARCHICAL ARCHIMEDEAN COPULAS (LSHAC) APPROACH

BY

WENJUN ZHU, KEN SENG TAN, LYSA PORTH AND CHOU-WEN WANG

ABSTRACT

Adverse weather-related risk is a main source of crop production loss and a big concern for agricultural insurers and reinsurers. In response, weather risk hedging may be valuable, however, due to basis risk it has been largely unsuccessful to date. This research proposes the Lévy subordinated hierarchical Archimedean copula model in modelling the spatial dependence of weather risk to reduce basis risk. The analysis shows that the Lévy subordinated hierarchical Archimedean copula model can improve the hedging performance through more accurate modelling of the dependence structure of weather risks and is more efficient in hedging extreme downside weather risk, compared to the benchmark copula models. Further, the results reveal that more effective hedging may be achieved as the spatial aggregation level increases. This research demonstrates that hedging weather risk is an important risk management method, and the approach outlined in this paper may be useful to insurers and reinsurers in the case of agriculture, as well as for other related risks in the property and casualty sector.

KEYWORDS

Systemic weather risk, hedging strategies, hierarchical Archimedean copulas, Lévy subordinators, agricultural insurance, reinsurance.

JEL codes: C13, C15, C16, G17, G22, Q19, Q14.

1. INTRODUCTION

Weather risk is described as the operational and financial variabilities caused by adverse meteorological conditions, and is a major environmental issue and a key economic factor. Possible changes in climate increase concerns of more frequent and severe extreme natural hazards occurring over larger areas and

Astin Bulletin 48(2), 779-815. doi: 10.1017/asb.2018.6 © 2018 by Astin Bulletin. All rights reserved.

Downloaded from https://www.cambridge.org/core. NTU Library, on 08 Jan 2020 at 04:20:35, subject to the Cambridge Core terms of use, available at https://www.cambridge.org/core/terms. https://doi.org/10.1017/asb.2018.6

affecting more people (IPCC, 2007; Hellmuth *et al.*, 2009). The Property & Casualty (P&C) insurance sector is highly focused on managing catastrophic losses due to extreme weather risk (Dong *et al.*, 1996; Priest, 1996; Odening and Shen, 2012), and the agriculture sector is one of the most exposed industries to weather-related risks. For example, some research estimates adverse weather may be responsible for at least 70% of agricultural loss, including crop and livestock production (USDA, 2014). Compared to other lines of business in the P&C sector, agricultural insurers and reinsurers have also been shown to bear higher loss ratios (Woodard and Garcia, 2008b), and this may become more pronounced in the future due to additional exposure to weather risk resulting from the increase of climate variability and uncertainty (Turvey *et al.*, 2006).

A major challenge facing the agricultural sector is that weather risk is systematic and undiversifiable in the sense that it is outside the control of human management, and at times weather risk can be widespread and spatially correlated, impacting many farms within a region (Woodard *et al.*, 2012; Porth *et al.*, 2015). Therefore, weather risk will not be eliminated by pooling, and must be managed through various risk transfer techniques. Agricultural insurance schemes have played an important role in helping to stabilize a producer's income by minimizing the economic effects caused by adverse weather events. To alleviate an insurer's exposure to large potential losses, private reinsurance is often purchased in addition to pooling to help diversify its portfolio of crop risks (Miranda and Glauber, 1997). For example, Porth *et al.* (2015) show that risk transfer (private reinsurance) is necessary in order to help ensure the solvency of crop insurance companies in Canada. Further, a study from Qatar Re shows that almost 80% of the global downside risk for agricultural insurers are reinsured (Schneider and Roth, 2013). In Canada, many of the provincial government crop insurance companies receive reinsurance protection from a unique Federal-Provincial Reinsurance Fund, and many provinces also purchase reinsurance from the private market. Similarly, in the United States, the private crop insurance companies receive reinsurance protection through the Standard Reinsurance Agreement, and many also purchase private reinsurance. Despite the important role that risk transfer plays in the sustainability of crop insurance programs, relatively little research has investigated optimal reinsurance strategies in the context of agriculture (see, for example, Porth *et al.*, 2013; 2015).

Beyond reinsurance, limited research has been conducted regarding efficient strategies to hedge systemic weather risk (see, for example, Woodard and Garcia, 2008b), and this may be valuable in the case of agriculture, as well as for other catastrophic weather risks that play a prominent role in the P&C sector. For example, some research has shown that introducing weather derivatives (WDs) into risk management policies leads to higher firm value (Pérez-González and Yun, 2013), and incorporating climate risk information has also been shown to improve the stock market efficiency (Hong *et al.*, 2016). While most of the WDs are customized products transacted over-the-counter, the organized markets are becoming more popular with many types of WDs traded on the Chicago Mercantile Exchange (CME). Therefore, one objective of this paper is to

Downloaded from https://www.cambridge.org/core. NTU Library, on 08 Jan 2020 at 04:20:35, subject to the Cambridge Core terms of use, available at https://www.cambridge.org/core/terms. https://doi.org/10.1017/asb.2018.6

develop and compare different weather risk hedging strategies for application to insurers and reinsurers, using agriculture as an example. A main focus of the research is on investigating the spatial dependence and aggregation level of systemic weather risks across a country and their impact on hedging.

In some cases, hedging weather risks with financial instruments may be advantageous over traditional reinsurance. Alternatively, it may be complimentary to private reinsurance in some cases, as part of an overall risk-layering framework, potentially reducing cost and improving market efficiency (Cummins *et al.*, 2004; Golden *et al.*, 2007). For example, financial instruments do not require loss checking and adjusting, thereby saving administration costs. Further, financial weather instruments may reduce information asymmetry, including adverse selection and moral hazard, which is a concern in crop insurance and reinsurance (Goodwin, 2001). This is because the indemnities of financial weather instruments are triggered based on a specific weather event rather than actual farm losses, which is a more transparent approach that is not subject to manipulation, etc. Furthermore, from a statistical inference viewpoint, the modelling and pricing of financial weather instruments may face less challenges, since large volumes of reliable and extensive weather data records are typically available in daily frequency. In contrast, agricultural underwriting is often faced with the challenge of shortness of data, given that only one yield or loss observation is recorded each year, and due to crop rotation and other factors, the time series may also suffer from missing data (Coble *et al.*, 2011; 2013; Porth *et al.*, 2014b). Therefore, weather hedging via financial engineering tools may provide new opportunities for risk management to the agricultural sector, including insurers and reinsurers.

In developing various weather risk hedging strategies, a focus of this research is on refining the statistical modelling of weather variables. This is an essential, yet, challenging task for financial weather instrument pricing and hedging, owing to the non-stationarity, seasonality and multidimensionality of the weather data (Dischel and Barrieu, 2002; Carriquiry and Osgood, 2012), as well as the incomplete nature of the market (Alexandridis and Zapranis, 2013). In this paper, Fourier series is used to capture the seasonalities in both the original temperature series as well as in the volatilities of the data, in addition to the exponential generalized autoregressive conditional heteroskedasticity (EGARCH(1,1)) process (Nelson, 1991). In addition, spatial dependence has been shown to be a critical factor in modelling weather risk and pricing WDs (Erhardt, 2015), and hence, has attracted substantial attention in the literature (Barth *et al.*, 2011; Šaltytė Benth and Šaltytė, 2011; Härdle and Osipenko, 2012; Benth and Benth, 2013; Okhrin *et al.*, 2013a; Erhardt and Smith, 2014; Erhardt, 2015). In particular, failure to consider the dependence structure for weather variable modelling and WD pricing may lead to substantial basis risk in the resulting hedging strategy if the spatial correlations are not taken into account. To overcome the high-dimensionality of the weather data and model the spatial dependence of weather events, this paper proposes a new copula family called the Lévy subordinated hierarchical Archimedean copula (LSHAC) model (Hering *et al.*, 2010; Mai and

Downloaded from https://www.cambridge.org/core. NTU Library, on 08 Jan 2020 at 04:20:35, subject to the Cambridge Core terms of use, available at https://www.cambridge.org/core/terms. https://doi.org/10.1017/asb.2018.6

Scherer, 2012; Zhu *et al.*, 2016; 2017). To the best of our knowledge, this is the first paper to employ the LSHAC for modelling the geographical dependence of weather events. The empirical results show that the proposed LSHAC model is successful in addressing the high-dimensional nature of weather risk modelling, providing better estimation compared to the Archimedean copula (AC) and traditional hierarchical Archimedean copula (HAC). Finally, in this paper, we also propose a pricing framework based on the conditional Esscher transform method (Gerber and Shiu, 1994; Bühlmann *et al.*, 1996) to address the challenge of instrument pricing in an incomplete market. In addition to basis risk, difficulties in pricing has also contributed to the unsuccessful implementation of weather risk hedging.

To examine the modelling framework proposed in this paper, an empirical analysis is conducted using 50 years temperature processes from eight provinces in Canada. The focus is on temperature, rather than precipitation because previous studies argue that temperature has a higher correlation with crop production compared to precipitation, therefore, making it better suited for crop insurance hedging (Lobell and Burke, 2008; Woodard and Garcia, 2008a). Using the refined statistical modelling of the weather data proposed in this paper, four hedging strategies are developed and compared. In assessing the effectiveness of the various hedging strategies, we are interested in the following three problems: (1) the necessity of hedging weather risk; (2) the importance of the assumed underlying dependence structure; (3) the geographical aggregation effect on hedging effectiveness. The results indicate that hedging weather risk is an important risk management approach, and the LSHAC model can improve the hedging performance through more accurate modelling of the dependence structure of weather risks. Moreover, the results reveal significant geographical aggregation benefits in weather risk hedging, which means that more effective hedging may be achieved as the spatial aggregation level increases.

The remainder of this paper is organized as follows. Section 2 briefly describes the proposed modes and the modelling methodology. In Section 3, the modelling and pricing procedure proposed preceding section is introduced in more detail using Canadian daily temperature data. Section 4 presents a simulation result on assessing the effectiveness of the various weather hedging strategies for insurers and reinsurers. Section 5 concludes the paper and Appendix A displays plots of standardized residuals.

2. General modelling framework

This section outlines the general modelling and pricing framework used in this paper to investigate the spatial dependence and aggregation level for developing an appropriate weather risk hedging approach. Figure 1 provides a snapshot of the proposed framework. An empirical application of this framework to Canada weather data will be presented in Section 3.

Downloaded from https://www.cambridge.org/core. NTU Library, on 08 Jan 2020 at 04:20:35, subject to the Cambridge Core terms of use, available at https://www.cambridge.org/core/terms. https://doi.org/10.1017/asb.2018.6

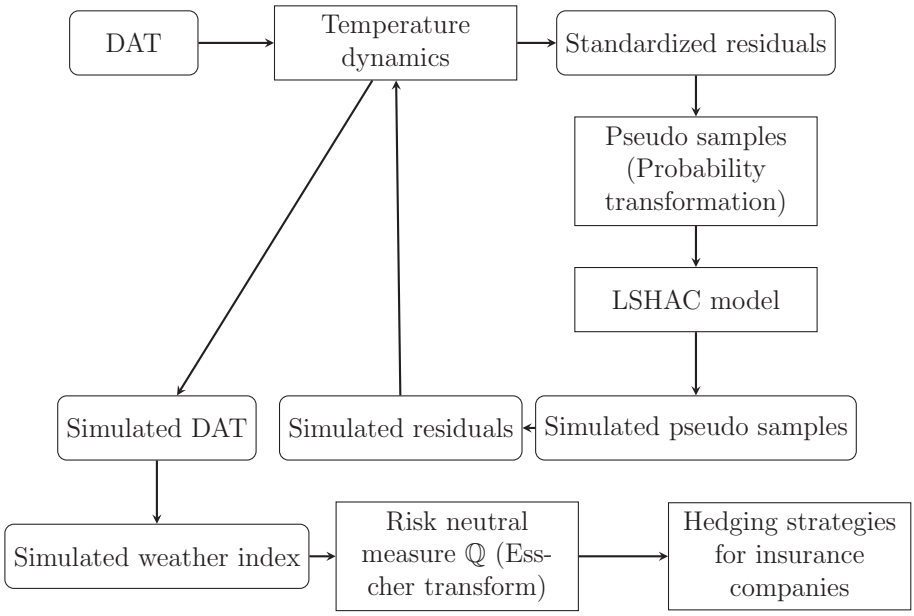


FIGURE 1: Flow chart of the general modelling framework.

The multivariate daily average temperature (DAT) model is constructed involving two steps. First, the marginal dynamic for each region i is analysed with Fourier series to capture the seasonalities in both the original temperature series as well as in the volatilities of the data, together with the EGARCH(1,1) process. Second, the dependence structure between different regions is constructed using a proposed LSHAC model, which is shown to have better estimation performance compared to the AC and HAC models. Next, the weather index data are simulated according to the estimated joint distribution, and the corresponding WDs are priced under a risk neutral measure. Finally, various weather hedging strategies are developed and their relative efficiencies are assessed.

2.1. Temperature dynamics

Let $Y_i(t)$ be the daily temperature (i.e. DAT) at time t in region i, $i = 1, \ldots, d$, where d denotes the total number of regions and t is measured in unit of days. Prompted by the non-stationarity and seasonality nature of the DAT, we adopt a model similar to that in Alexandridis and Zapranis (2013), Okhrin *et al.* (2013a), Campbell and Diebold (2005), Dupuis (2012; 2014), i.e. by assuming the dynamics of $Y_i(t)$ can be modelled by the sum of the following three components:

$$Y_i(t) = \Gamma_i(t) + \Pi_i(t) + \Upsilon_i(t), \tag{1}$$

Downloaded from https://www.cambridge.org/core. NTU Library, on 08 Jan 2020 at 04:20:35, subject to the Cambridge Core terms of use, available at https://www.cambridge.org/core/terms. https://doi.org/10.1017/asb.2018.6

where the deterministic trend Γ_i is modelled by the linear function with coefficients $(\gamma_{0,i}, \gamma_{1,i}; i = 1, \ldots, d)$:

$$\Gamma_i(t) = \gamma_{0,i} + \gamma_{1,i}\frac{t}{365}, \tag{2}$$

the seasonality factor Π_i is modelled by K sine and cosine Fourier terms with coefficients $(a_{k,i}, b_{k,i}; k = 1, \ldots, K, i = 1, \ldots, d)$ and a repeating step function $d(t)$ that cycles through $1, \ldots, 365$ (we drop February 29 for all leap years):

$$\Pi_i(t) = \sum_{k=1}^{K}\left(a_{k,i}\sin\left(2\pi k\frac{d(t)}{365}\right) + b_{k,i}\cos\left(2\pi k\frac{d(t)}{365}\right)\right), \tag{3}$$

and the cyclical dynamics of the data Υ_i is captured by L autoregressive lags with parameters $(\rho_{l,i}; l = 1, \ldots, L, i = 1, \ldots, d)$:

$$\Upsilon_i(t) = \sum_{l=1}^{L}\rho_{l,i}\, Y_i(t-l) + \sigma_i(t)z_i(t). \tag{4}$$

Here, $z_i(t)$ is a stationary iid process with mean 0 and variance 1 and the residual volatility $\sigma_i(t)$ is modelled by

$$\begin{aligned}\log\sigma_i^2(t) = \omega_i + \xi_i\Big(|z_i(t-1)| - \mathrm{E}(|z_i(t-1)|)\Big) + \kappa_i z_i(t-1) + \eta_i\log\sigma_i^2(t-1) \\ + \sum_{s=1}^{S}\left(\alpha_{s,i}\sin\left(2\pi s\frac{d(t)}{365}\right) + \beta_{s,i}\cos\left(2\pi s\frac{d(t)}{365}\right)\right).\end{aligned} \tag{5}$$

After removing the trend as well as seasonal and cyclical effects, the logarithm of the residual conditional variance is modelled by an exponential generalized autoregressive conditional heteroskedasticity (EGARCH(1,1)) process (Nelson, 1991), together with an additional leverage term to capture asymmetric volatility clustering in the daily temperature (Dupuis, 2014). More specifically, it contains a GARCH coefficient, η_i, associated with a lagged log variance term, an ARCH coefficient, ξ_i, associated with the magnitude of lagged standardized innovations, and a leverage coefficient, κ_i, associated with the signed, lagged standardized innovations. Furthermore, when modelling the temperature residual volatility in Equation (5), we also add S sine and cosine terms to capture the seasonality of the volatility.

In the empirical estimation to be discussed in Section 3, parameters are obtained using the following two-stage estimation procedure:

1. Apply the least square estimation method to Equations (2) and (3), i.e., the coefficients of the trend $(\gamma_{0,i}, \gamma_{1,i}; i = 1, \ldots, d)$ and seasonality $(a_{k,i}, b_{k,i}; k = 1, \ldots, K, i = 1, \ldots, d)$.

Downloaded from https://www.cambridge.org/core. NTU Library, on 08 Jan 2020 at 04:20:35, subject to the Cambridge Core terms of use, available at https://www.cambridge.org/core/terms. https://doi.org/10.1017/asb.2018.6

2. Use the maximum likelihood estimation method to calibrate Equations (4) and (5), i.e., the cyclical lags $(\rho_{l,i}; l = 1, \ldots, L, i = 1, \ldots, d)$ and the volatility parameters $\omega_i, \xi_i, \kappa_i, \eta_i, \alpha_{s,i}, \beta_{s,i}; s = 1, \ldots, S; i = 1, \ldots, d$.[1]

2.2. Spatial temperature modelling with LSHAC

Recall that a key objective of this paper is to construct an efficient way of hedging weather risk across various regions. A multivariate model that adequately captures the spatial dependence of weather variables is of paramount importance in minimizing the spatial basis risk, and hence leads to a more effective hedging strategy. The preceding section postulates a plausible (marginal) distribution for modelling weather data for a single region. By taking into consideration the trend, the seasonality and the cyclicality of the inherent nature of the weather data, we obtain the stationary process $z_i(t)$ with mean 0 and variance 1 for regions $i = 1, \ldots, d$. The next step is to conduct the probability transformation to $z_i(t)$ and get the pseudo samples, $\boldsymbol{u} = (u_1, \ldots, u_d)'$. This in turn facilitates us in utilizing the copula method (Joe, 1997) to create a joint distribution of weather data.

Copula models have been widely used in the area of risk management and the design and pricing of insurance contracts (see, for example, McNeil *et al.*, 2010; Avanzi *et al.*, 2011; Shi and Frees, 2011; Arbenz and Canestraro, 2012; Embrechts and Hofert, 2013; Goodwin and Hungerford, 2014; Shi, 2014; Hürlimann, 2014; Abdallah *et al.*, 2015; Yang *et al.*, 2015; Chuliá *et al.*, 2016).

One of the popular copulas is known as the AC. AC provides a convenient way of modelling high-dimensional dependence due to its simplicity, involving only one parameter. Let $C : [0, 1]^d \to [0, 1]$ be a d-dimensional AC defined as

$$C(u_1, u_2, \ldots, u_d) = \psi\left(\psi^{-1}(u_1) + \cdots + \psi^{-1}(u_d)\right), \tag{6}$$

where $\psi \in \mathcal{G} = \{\psi : [0, \infty) \to [0, 1] \mid \lim_{u\to\infty} \psi(u) = 0, \psi(0) = 1, (-1)^k \frac{d^k}{du^k}\psi(u) \geq 0, k \in \mathbb{N}\}$, is called the completely monotonic (c.m.) generator and ψ^{-1} is its inverse, defined as $\psi^{-1}(u) = \inf\{t : \psi(t) \leq u\}$. In view of Equation (6), the distributions of $u_1, u_2, \ldots, u_d$ are invariant upon permutation, and this exchangeable structure severely restricts the modelling capability of AC models.

The HAC, which nests random variables into a hierarchy, has been proposed to address the problem of exchangeability. A general modelling framework and properties of the HAC is given by Savu and Trede (2010). Sampling algorithms for the HAC are provided by Whelan (2004) and McNeil (2008). Estimation is developed by Savu and Trede (2010) for the HAC with a known structure, and Okhrin *et al.* (2013b) for the HAC with a recursive estimation procedure. The HAC models are applied to determine the spatial dependence of weather events in China by Okhrin *et al.* (2013a). Although more general and flexible, there are compatible conditions that are very difficult to check empirically to ensure

Downloaded from https://www.cambridge.org/core. NTU Library, on 08 Jan 2020 at 04:20:35, subject to the Cambridge Core terms of use, available at https://www.cambridge.org/core/terms. https://doi.org/10.1017/asb.2018.6

that the resulting HAC yields a valid copula function. As a result, almost all applications of the HAC models rely on the Gumbel copula (GM) or the Clayton copula (CL), which have been verified to fulfil the compatible conditions. However, if the HAC models are constructed from mixed generators involving different families, one must verify the compatible conditions on a case-by-case basis, which significantly restricts the empirical application of the HAC models (Embrechts *et al.*, 2003).

In view of the aforementioned difficulties, Hering *et al.* (2010) circumvent this hard-to-check compatible condition by constructing the HAC models via Lévy Subordinators. Mai and Scherer (2012) include the LSHAC model in a h-extendible framework. Zhu *et al.* (2016) provide the estimation methodology and empirically test the efficiency of the LSHAC models. The advantage of this model is that c.m. generators constructed with Lévy subordinators automatically satisfy the compatible conditions. For a thorough review of Lévy processes, refer to Tankov (2004). LSHAC models enlarge the HAC family, flexible in modelling the tail dependence and are suitable to construct different hierarchical structures depending on the properties of the data. Therefore, in this paper, we utilize the LSHAC model to estimate the dependence structure of the spatial temperature process. This is the first paper to use the LSHAC for modelling the geographical dependence of weather events. The empirical results in Section 3 show that the LSHAC models have better estimation performance compared to ACs and HAC models.

2.3. Esscher transform and pricing formulas

When the market is complete, a unique risk neutral measure can be obtained by changing the process of the underlying asset into a martingale, and the securities can be priced as the expectation of the discounted derivative payoff under the risk neutral measure. However, the WD market is incomplete and there exists more than one equivalent risk neutral measure (Tankov, 2004). Therefore, traditional arbitrage-free theory cannot be applied in pricing securities written on weather indices, since the underlying assets cannot be traded.

The pricing methodology employed in this paper uses a martingale measure based on the conditional Esscher transform (Bühlmann *et al.*, 1996; Gerber and Shiu, 1994), which has been widely used in financial and insurance securities pricing in incomplete markets (Siu *et al.*, 2004; Li *et al.*, 2010; Yang, 2011). We define a $\mathcal{F}_t$-adapted stochastic process $\{\zeta_t | t = 1, 2, \ldots, T\}$ as follows:

$$\zeta_T = \prod_{t=1}^{T} \frac{\exp\big(\theta\, Y(t)\big)}{E^{\mathbb{P}}\big(\exp(\theta\, Y(t))|\mathcal{F}_{t-1}\big)}, \tag{7}$$

where θ is the parameter of the Esscher transform representing the market price of risk (MPR) charged for the WDs. Usually, θ describes the risk preferences of policyholders. Hence, a new martingale measure with respect to θ, $\mathbb{Q}_\theta$, can be

Downloaded from https://www.cambridge.org/core. NTU Library, on 08 Jan 2020 at 04:20:35, subject to the Cambridge Core terms of use, available at https://www.cambridge.org/core/terms. https://doi.org/10.1017/asb.2018.6

defined as

$$\frac{d\mathbb{Q}_\theta}{d\mathbb{P}} \mid_{\mathcal{F}_T} = \zeta_T. \tag{8}$$

The Esscher transform has several advantages. First and foremost, the Esscher transform changes the jump size (i.e., the price of jump risk) of the process under $\mathbb{Q}_\theta$ (Tankov, 2004; Hubalek and Neilsen, 2006). Second, the Esscher transform leads to a minimal entropy martingale measure in certain situations, which is closest to the original physical measure (Frittelli, 2000; Tankov, 2004; Hubalek and Neilsen, 2006). Finally, many distributions stay invariant under the Esscher transform in the sense that their density functions retain their original form. This makes the Esscher transform easy to obtain and apply for pricing in a practical sense.

3. Empirical analysis of weather risk in Canada

In this section, we analyse the systemic weather risk in Canada following the modelling framework described in Section 2. First, the dataset used in this study is described in Section 3.1. Next, the marginal dynamics and spatial dependence of the data are estimated and analysed in Section 3.2.

3.1. Data

The DAT data used in this paper includes the Adjusted and Homogenized Canadian Climate data, obtained from Environment Canada covering 50 years from 1962 to 2011. This dataset contains daily temperature series for eight provinces in Canada, including Alberta (AB), Saskatchewan (SK), British Columbia (BC), Manitoba (MB), Ontario (ON), New Brunswick (NB), Nova Scotia (NS) and Quebec (QC). The geographical locations of these provinces are pictured in Figure 2. These eight provinces were selected because they contain more than 98.72% of the farms and 99.26% of the aggregate farm incomes in Canada, and include most agricultural insurance programs in Canada. In addition, there are six WD trading cities among these eight provinces, including Calgary (AB), Edmonton (AB), Vancouver (BC), Toronto (ON), Montreal (QC) and Winnipeg (MB).

The descriptive statistics of DAT for the eight provinces are summarized in Table 1. We observe that the weather risk conditions vary across the provinces. For example, the 0.01 quantile of temperature is $-29.75\,^{\circ}$C in MB, while in BC, it is $-15.39\,^{\circ}$C. A good understanding of the heterogeneity of weather risks across provinces provides an opportunity for insurers and reinsurers to diversify their risk portfolios and develop efficient hedging strategies.

Downloaded from https://www.cambridge.org/core. NTU Library, on 08 Jan 2020 at 04:20:35, subject to the Cambridge Core terms of use, available at https://www.cambridge.org/core/terms. https://doi.org/10.1017/asb.2018.6

TABLE 1

DESCRIPTIVE STATISTICS OF CANADA'S DAT (IN CELSIUS) FROM 1962 TO 2011 FOR PROVINCES ALBERTA (AB), SASKATCHEWAN (SK), BRITISH COLUMBIA (BC), MANITOBA (MB), ONTARIO (ON), NEW BRUNSWICK (NB), NOVA SCOTIA (NS), AND QUEBEC (QC). THE FOLLOWING STATISTICS ARE REPORTED: MEAN, STANDARD DEVIATION (SD), SKEWNESS, KURTOSIS, QUANTILES Q_α, FOR $\alpha \in \{1\%, 5\%, 95\%, 99\%\}$.

	AB	BC	MB	NB	NS	ON	QC	SK
Mean	−1.44	4.49	0.84	2.50	4.98	1.49	−1.49	−1.02
SD	6.83	5.58	14.28	8.15	7.14	8.35	6.59	9.10
Skewness	−1.60	−1.61	−0.39	−0.54	−0.45	−0.93	−1.03	−1.26
Kurtosis	6.11	6.38	2.05	3.37	2.57	3.08	3.86	4.34
$Q_{0.01}$	−25.82	−15.39	−29.75	−19.57	−12.74	−20.88	−20.83	−29.25
$Q_{0.05}$	−16.02	−6.64	−24.38	−13.40	−7.90	−15.24	−15.29	−20.90
$Q_{0.95}$	6.06	10.59	19.73	14.70	14.81	11.24	6.97	9.57
$Q_{0.99}$	8.18	12.33	22.36	19.04	16.86	13.48	9.85	11.99



FIGURE 2: Map of Canada by provinces. (Color online)

3.2. Empirical estimation results

In this section, the statistical framework described in Section 2 is applied to the Canada's DAT. Based on the estimation method and the assumptions provided in Section 2, the marginal parameters from Equations (1)–(5) are calibrated. In particular, $K = S = 5$ are selected based on the Bayesian information criterion (BIC), and a large value of $L = 25$ to capture the long-memory dynamics of the data, following Campbell and Diebold (2005). The estimation results are displayed in Tables 2 and 3. As we can see from these results, the parameters associated with the trend and seasonality are mostly significant, even at 1%.[2]

Downloaded from https://www.cambridge.org/core. NTU Library, on 08 Jan 2020 at 04:20:35, subject to the Cambridge Core terms of use, available at https://www.cambridge.org/core/terms. https://doi.org/10.1017/asb.2018.6

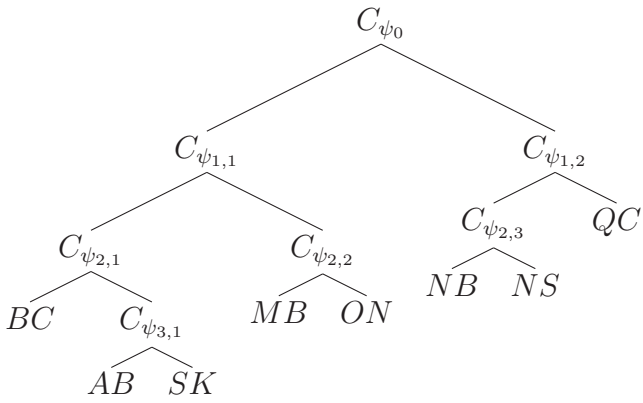


FIGURE 3: Hierarchical structure of the temperature process for eight Canadian provinces.

Note that only standard errors (instead of t-statistics tests as in Table 2) from the second-stage estimation are displayed in Table 3. The plots and histograms of standardized residuals of marginal distributions depicted in Appendix A are also reasonable.

We next consider the spatial dependence of the temperature process, which will be modelled via the LSHAC model. To estimate the LSHAC model, we first need to determine its hierarchical structure. We achieve this via the hierarchical clustering analysis.[3] The resulting structure is displayed in Figure 3 and it can be described as follows:[4]

- The structure emanates from the outer copula (C_{ψ_0}) at level 0.
- At level 1, the structure is classified into two subgroups:
  - The first subgroup contains five provinces in the west and central territories of Canada (including BC, AB, SK, MB and ON), and is nested together into the inner copula $C_{\psi_{1,1}}$.
  - The second subgroup contains three provinces in the east (including NB, NS and QC), and is nested into $C_{\psi_{1,2}}$.
- At level 2, provinces from the west, central and east parts of Canada are grouped in to different subgroups:
  - Western provinces (including BC, AB and SK) are nested together by $C_{\psi_{2,1}}$.
  - Central provinces (including MB and ON) are grouped together by $C_{\psi_{2,2}}$.
  - Eastern provinces NB and NS are first nested together by $C_{\psi_{2,3}}$, and then grouped into $C_{\psi_{1,2}}$ with QC.
- At level 3, AB and SK are nested together into the inner copula $C_{\psi_{3,1}}$.

Note that the hierarchal structure given in Figure 3 is consistent with our intuition, the grouping corresponds to the geographical positioning of the eight provinces as shown in Figure 2. For example, BC, AB and SK are three neighbouring provinces in the western part of Canada, and are grouped together. The two provinces in central Canada, MB and ON, are in the same subgroup. The

Downloaded from https://www.cambridge.org/core. NTU Library, on 08 Jan 2020 at 04:20:35, subject to the Cambridge Core terms of use, available at https://www.cambridge.org/core/terms. https://doi.org/10.1017/asb.2018.6

Downloaded from https://www.cambridge.org/core. NTU Library, on 08 Jan 2020 at 04:20:35, subject to the Cambridge Core terms of use, available at https://www.cambridge.org/core/terms. https://doi.org/10.1017/asb.2018.6

TABLE 2

ESTIMATION RESULTS FOR TREND AND SEASONALITIES OF THE TEMPERATURE PROCESSES FROM EIGHT PROVINCES IN CANADA.

	AB	BC	MB	NB	NS	ON	QC	SK
γ_0	−0.4008***	0.5497***	0.0077	0.1709	1.2334***	0.0805**	−0.6440***	−0.2989*
	(−6.1949)	(5.6363)	(0.9779)	(0.5585)	(9.2569)	(2.1018)	(−8.1870)	(−1.6322)
γ_1	0.0069***	0.0046**	0.0052***	0.0129*	0.0096***	0.0085***	0.0118***	0.0059
	(3.3348)	(2.1192)	(6.5826)	(1.5110)	(4.8826)	(4.6717)	(4.8042)	(0.6624)
a_1	−0.5287***	−0.4997***	−0.5980***	−0.5159***	−2.0170***	−1.2076***	−0.6833***	−0.6261**
	(−13.7720)	(−3.6025)	(−4.5120)	(−3.2592)	(−8.7616)	(−13.1300)	(−10.1789)	(−2.2041)
a_2	−0.6826***	−0.3067***	−0.0591*	−0.4222***	−0.1791***	−0.6498***	−0.9943***	−0.5182***
	(−20.0283)	(−5.3970)	(−1.6660)	(−7.2132)	(−3.4302)	(−16.5442)	(−18.3130)	(−8.0884)
a_3	−0.2620***	−0.2192***	−0.0305*	−0.5499***	−0.2624***	−0.2727***	−0.2618***	−0.4039***
	(−9.7751)	(−5.1215)	(−1.5207)	(−7.8703)	(−8.4693)	(−5.8027)	(−10.1954)	(−10.5486)
a_4	−0.2996***	−0.1368***	0.0869***	−0.2309***	−0.1957***	−0.2771***	−0.3729***	−0.1395***
	(−11.2673)	(−2.4942)	(2.4261)	(−3.6448)	(−5.3594)	(−7.3879)	(−12.4646)	(−3.2425)
a_5	−0.2321***	−0.1489***	0.0299	−0.0984**	−0.1674***	−0.2016***	−0.1616***	−0.1596
	(−10.8223)	(−8.5903)	(0.5983)	(−1.8075)	(−5.6869)	(−10.0537)	(−3.1475)	(−0.4629)
b_1	−0.5773***	−0.7336***	−3.0324***	−1.8110***	−1.8133***	−1.6122***	−1.3150***	−1.4010***
	(−17.0991)	(−6.0453)	(−21.6726)	(−12.2987)	(−18.6990)	(−21.1921)	(−18.9708)	(−7.3192)
b_2	−0.0690***	−0.0652	−0.2830***	−0.1305*	−0.3357***	−0.1222***	0.0757	−0.1391***
	(−2.9722)	(−0.8347)	(−8.5661)	(−1.3778)	(−11.3798)	(−4.3676)	(1.1964)	(−2.9171)
b_3	−0.1569***	−0.1146***	−0.0673	−0.3568***	−0.0187**	0.0148*	0.0671**	−0.0974
	(−6.6929)	(−5.4422)	(−0.6067)	(−6.4060)	(−1.8564)	(1.5786)	(1.7236)	(−0.4371)
b_4	−0.0851***	−0.0923***	0.0243***	0.1721**	0.0301	−0.0808***	−0.0306***	−0.0554
	(−2.9107)	(−2.6565)	(2.6040)	(1.7412)	(1.1035)	(−3.5836)	(−2.6599)	(−0.5106)
b_5	−0.0418**	−0.0064	0.0311	−0.2742***	0.1047***	0.0213***	0.0192	−0.0518
	(−1.9540)	(−0.2568)	(0.6119)	(−3.5671)	(2.7798)	(3.2318)	(0.6352)	(−0.3869)

Values of t statistics are displayed in the parentheses. "***" means significant at 0.01 level, "**" means significant at 0.05 level, and "*" means significant at 0.1 level.

TABLE 3

ESTIMATION RESULTS FOR VOLATILITIES OF THE TEMPERATURE PROCESSES FROM EIGHT PROVINCES IN CANADA.

	AB	BC	MB	NB	NS	ON	QC	SK
ω	0.3951	0.0680	0.4229	0.5216	0.5616	0.2451	0.3697	0.4145
	[0.0314]	[0.0023]	[0.0169]	[0.0555]	[0.0799]	[0.0238]	[0.0274]	[0.0179]
ξ	0.0889	0.2036	0.0379	0.0578	0.0920	0.0502	0.0934	0.0645
	[0.0066]	[0.0117]	[0.0040]	[0.0054]	[0.0050]	[0.0057]	[0.0070]	[0.0017]
η	0.6722	0.4252	0.7539	0.7313	0.5128	0.7696	0.6692	0.6672
	[0.0220]	[0.1960]	[0.0513]	[0.0743]	[0.0450]	[0.0168]	[0.0169]	[0.0226]
κ	0.0460	−0.0018	0.0178	0.0147	0.0617	0.0445	0.0595	0.0314
	[0.0045]	[0.0004]	[0.0055]	[0.0019]	[0.0069]	[0.0027]	[0.0030]	[0.0087]
α_1	0.1147	0.1717	−0.0108	0.0554	0.1676	0.0504	0.0753	0.0917
	[0.0076]	[0.0440]	[0.0015]	[0.0147]	[0.0272]	[0.0037]	[0.0062]	[0.0326]
α_2	0.0472	0.0334	0.0133	−0.0183	0.0120	−0.0047	0.0551	0.0323
	[0.0069]	[0.0053]	[0.0045]	[0.0029]	[0.0032]	[0.0010]	[0.0075]	[0.0068]
α_3	−0.0352	−0.0776	−0.0175	0.0046	0.0080	−0.0299	−0.0003	−0.0359
	[0.0019]	[0.0203]	[0.0092]	[0.0015]	[0.0003]	[0.0044]	[0.0000]	[0.0038]
α_4	−0.0639	−0.0373	0.0118	−0.0062	0.0296	−0.0162	−0.0442	−0.0382
	[0.0055]	[0.0035]	[0.0014]	[0.0003]	[0.0138]	[0.0025]	[0.0050]	[0.0051]
α_5	−0.0731	−0.2010	0.0116	−0.0062	−0.0999	−0.0305	−0.0356	−0.0236
	[0.0250]	[0.0630]	[0.0038]	[0.0015]	[0.0114]	[0.0083]	[0.0064]	[0.0072]
β_1	0.1400	0.3361	0.1672	0.0669	0.2937	0.1074	0.1000	0.2232
	[0.0031]	[0.0601]	[0.0180]	[0.0157]	[0.0427]	[0.0151]	[0.0024]	[0.0788]
β_2	0.1536	0.2572	−0.0030	0.0809	0.1310	0.1127	0.1796	0.1249
	[0.0100]	[0.0664]	[0.0001]	[0.0115]	[0.0033]	[0.0124]	[0.0124]	[0.0239]
β_3	0.1103	0.1675	0.0153	0.0586	0.0998	0.0456	0.0606	0.0696
	[0.0280]	[0.0592]	[0.0017]	[0.0072]	[0.0147]	[0.0066]	[0.0052]	[0.0097]
β_4	0.0210	0.0454	−0.0160	−0.0105	0.0711	0.0108	0.0190	0.0298
	[0.0025]	[0.0071]	[0.0020]	[0.0015]	[0.0127]	[0.0020]	[0.0079]	[0.0029]
β_5	−0.0174	0.0226	−0.0037	−0.0122	−0.0287	−0.0015	0.0287	0.0171
	[0.0026]	[0.0043]	[0.0006]	[0.0029]	[0.0053]	[0.0002]	[0.0072]	[0.0027]

Standard errors are displayed in the square brackets below.

three provinces in the eastern part of Canada, namely, QC, NB and NS, are grouped together into another subgroup. This hierarchical structure provides information about weather risks in different geographical regions. In addition, this structure also indicates similar relationships between different provinces. The correlation matrix of the pseudo samples obtained following Section 2.2 is produced in Table 4. We can see that weather risks in regions within the same subgroup are more closely related compared to regions in other subgroups. This implies that it is important for insurance companies to consider the dependence structure of the risk portfolio they hold in order to develop any targeted hedging strategies.

According to Theorem 2.1 of Hering *et al.* (2010), the copulas at each node can be constructed by composing an outer copula to the Lévy subordinator.

Downloaded from https://www.cambridge.org/core. NTU Library, on 08 Jan 2020 at 04:20:35, subject to the Cambridge Core terms of use, available at https://www.cambridge.org/core/terms. https://doi.org/10.1017/asb.2018.6

TABLE 4

CORRELATION MATRIX OF PSEUDO SAMPLES OF PROVINCES TRANSFORMED FROM TEMPERATURE DATA.

	AB	BC	MB	NB	NS	ON	QC	SK
AB	1.00							
BC	0.44	1.00						
MB	0.06	−0.05	1.00					
NB	0.07	0.05	−0.09	1.00				
NS	0.08	0.06	−0.04	0.42	1.00			
ON	0.02	0.05	0.10	0.00	−0.05	1.00		
QC	0.10	0.10	−0.09	0.47	0.29	0.27	1.00	
SK	0.51	0.24	0.35	0.05	0.07	−0.01	0.05	1.00

TABLE 5

GENERATOR FUNCTIONS, UPPER TAIL DEPENDENCE (λ_u) AND LOWER TAIL DEPENDENCE (λ_l) OF ARCHIMEDEAN COPULA GENERATORS.

Family	$\psi(u)$	λ_u	λ_l	Parameter
GM	$\psi_{GM}(u) = \exp\left(-x^{\frac{1}{\theta}}\right)$	$2-2^{\frac{1}{\theta}}$	0	$\theta \geq 1$
CL	$\psi_{CL}(u) = (1+u)^{-\frac{1}{\theta}}$	0	$2^{-\frac{1}{\theta}}$	$\theta > 0$

CL: Clayton family, GM: Gumbel family.

TABLE 6

EXAMPLES OF LÉVY SUBORDINATORS.

Subordinator	$\Psi(u)$	Parameters
G	$\Psi_G = a\log(1+u/b)$	$a > 0, b > 0$
St	$\Psi_{St} = u^a$	$a > 1$
IG	$\Psi_{IG} = a\sqrt{2u+b^2} - ab$	$a > 0, b > 0$

G: Gamma process, St: Stable process, IG: Inverse Gaussian process.

Therefore, the LSHACs are highly flexible with a large number of candidate models. For example, in the modelling of this paper, the outer copulas of the LSHAC are selected as a GM or CL as listed in Table 5. The Lévy subordinators are chosen from the three processes listed in Table 6, including Gamma process (G), Stable process (St) and the Inverse Gaussian process (IG). As a consequence, to calibrate the eight-dimensional LSHAC model with seven AC generators in Figure 3, we have $2 \times 3^6 = 1,458$ models to choose from. Instead of going through all of the combinations, the estimation begins from the second level of the structure (i.e., start from estimating the optimal copulas of $C_{\psi_{2,1}}$, $C_{\psi_{2,2}}$, $C_{\psi_{2,3}}$ and $C_{\psi_{3,1}}$), and the St copula is found to provide the best fit. Therefore, the Lévy subordinators for $C_{\psi_{2,1}}$, $C_{\psi_{2,2}}$, $C_{\psi_{2,3}}$ and $C_{\psi_{3,1}}$ are fixed as St, reducing the candidate models to 18. It is important to emphasize that the GM and CL generators are selected for the outer copula in order to model

Downloaded from https://www.cambridge.org/core. NTU Library, on 08 Jan 2020 at 04:20:35, subject to the Cambridge Core terms of use, available at https://www.cambridge.org/core/terms. https://doi.org/10.1017/asb.2018.6

the asymmetric tail dependence of the data. For example, conditional on an extreme low temperature in MB, the neighbouring province of ON is highly probable to have a very low temperature too, indicating a lower tail dependence property. Similarly, an upper tail dependence means that extreme high temperatures tend to appear together for neighbouring provinces. The GM copula has upper tail dependence and the CL copula has lower tail dependence, as shown in the third and fourth columns in Table 5. Therefore, the LSHAC models potentially have the ability to capture the clusters of the extreme values in the data.

The estimation results are displayed in Table 7. The first seven columns describe the LSHAC model, particularly how to choose the ACs at each node. The first nine LSHAC models are constructed with the GM as their outer generators (denoted as GM–LSHAC), and the last nine LSHAC models are constructed with the CL as their outer generators (denoted as CL–LSHAC). Of interest, the first LSHAC model in Table 7 degenerates to the case of the traditional All–GM–HAC model. The log-likelihood function values (LLF), as well as the BIC values for each model are shown in the subsequent two columns. In our analysis, we use the AC, including GM and CL, as benchmarks. The improvements in BIC of the LSHAC models compared to the HAC (BIC Imp) are also displayed. In particular, a positive sign indicates better performance, while a negative sign indicates worse performance. The last column in the table shows the number of parameters in each copula model (# Para.). We obtain the following information based on the estimation results:

- The first LSHAC model in the table, which is highlighted in bold with a "†", is constructed in such a way that the copula at each node in the structure in Figure 3 is a GM generator, denoted as All–GM–HAC. This is currently the most common HAC model used in empirical analysis, such as Okhrin *et al.* (2013a), which uses an All–GM–HAC model to estimate the dependence structure of the temperature process in China. However, the estimation ability of this model is limited, and all except one of the LSHAC models in Table 7 are superior to this model. This is mainly because it restricts the copula at each node of the structure as a GM copula. Therefore, this paper introduces a more flexible LSHAC model with a large number of candidates to improve the estimation.
- Based on BIC values, all LSHAC models perform better than the AC, and most of the estimated LSHAC's are better than the traditional All–GM–HAC. In particular, the best LSHAC model has a 310.94 improvement in BIC, and is constructed with the CL copula as the outer generator, G Lévy subordinator for the first copula in the first level, and St Lévy subordinator for the remainder of the copulas in the structure. It is highlighted in bold with a "⋆" in the parentheses, and its structure is displayed in Figure A5 of Appendix B. In particular, details of the copula structure with the corresponding seven AC generators are displayed in Equations (B.1)–(B.8) of Appendix B.

Downloaded from https://www.cambridge.org/core. NTU Library, on 08 Jan 2020 at 04:20:35, subject to the Cambridge Core terms of use, available at https://www.cambridge.org/core/terms. https://doi.org/10.1017/asb.2018.6

TABLE 7

LSHAC ESTIMATION RESULTS FOR THE EIGHT-DIMENSIONAL HIERARCHICAL STRUCTURE IN FIGURE 3.

Archimedean Copula							LLF	BIC	BIC Imp.	# Para.
Gumbel Copula (GM)							912.82	−908.72	–	1
Clayton Copula (CL)							1306.83	−1303.73	–	1
LSHAC Model										
C_{ψ_0}	$C_{\psi_{11}}$	$C_{\psi_{12}}$	$C_{\psi_{21}}$	$C_{\psi_{22}}$	$C_{\psi_{23}}$	$C_{\psi_{31}}$	LLF	BIC	BIC Imp.	# Para.
GM	**St**	**St**	**St**	**St**	**St**	**St**	2145.47	**−2132.47**†	–	7
GM	**St**	**IG**	**St**	**St**	**St**	**St**	2199.08	−2145.76	+14.29	8
GM	**St**	**G**	**St**	**St**	**St**	**St**	2083.23	−2029.91	−102.56	8
GM	**IG**	**St**	**St**	**St**	**St**	**St**	2346.85	−2293.53	+161.06	8
GM	**IG**	**IG**	**St**	**St**	**St**	**St**	2411.04	−2357.73	+225.26	9
GM	**IG**	**G**	**St**	**St**	**St**	**St**	2283.11	−2229.79	+97.32	9
GM	**G**	**St**	**St**	**St**	**St**	**St**	2362.44	−2309.12	+176.65	8
GM	**G**	**IG**	**St**	**St**	**St**	**St**	2426.77	−2373.45	+240.98	9
GM	**G**	**G**	**St**	**St**	**St**	**St**	2298.63	−2245.31	+112.84	9
CL	**St**	**St**	**St**	**St**	**St**	**St**	2466.08	−2245.31	+112.84	7
CL	**St**	**IG**	**St**	**St**	**St**	**St**	2422.83	−2369.51	+237.04	8
CL	**St**	**G**	**St**	**St**	**St**	**St**	2288.64	−2235.32	+102.85	8
CL	**IG**	**St**	**St**	**St**	**St**	**St**	2496.16	−2442.84	+310.37	8
CL	**IG**	**IG**	**St**	**St**	**St**	**St**	2440.12	−2386.80	+254.33	9
CL	**IG**	**G**	**St**	**St**	**St**	**St**	2319.58	−2266.26	+133.79	9
CL	**G**	**St**	**St**	**St**	**St**	**St**	2496.73	**−2443.41**⋆	+310.94	8
CL	**G**	**IG**	**St**	**St**	**St**	**St**	2458.30	−2404.98	+272.51	9
CL	**G**	**G**	**St**	**St**	**St**	**St**	2320.20	−2266.88	+134.41	9

The first seven columns describe copulas at each node in the LSHAC model. The next column refers to the log-likelihood function values of different models (LLF), the Bayesian Information Criterion (BIC) is shown next, followed by the improvement in BIC of the LSHAC models compared to the first LSHAC, i.e., traditional All–GM–HAC model (BIC Imp.). In particular, a positive sign indicates better performance relative to the All–GM–HAC, while a negative sign indicates worse performance. The last column shows the number of parameters in each copula model (# Para.). The first nine LSHAC models are constructed with the GM as their outer generators (denoted as GM–LSHAC), and the last nine LSHAC models are constructed with the CL as their outer generators (denoted as CL–LSHAC). All–GM–HAC is highlighted in bold with a "†". The BIC of the best model is highlighted in bold with a "⋆" in the parentheses.

- Finally, comparing the results of the GM–LSHAC models and the CL–LSHAC models, the CL–LSHAC models are found to perform slightly better. This may be explained by the difference in the tail dependence properties. To be more specific, the CL copula, as shown in Table 5, has lower tail dependence, meaning that it can capture clustering of extreme low temperatures. In contrast, the GM copula only has upper tail dependence. The results show that lower tail dependence models (i.e., CL–LSHAC models) have better fitting results, indicating that the clustering of extreme low temperatures may be more important than extreme high temperature in Canada.

Downloaded from https://www.cambridge.org/core. NTU Library, on 08 Jan 2020 at 04:20:35, subject to the Cambridge Core terms of use, available at https://www.cambridge.org/core/terms. https://doi.org/10.1017/asb.2018.6

4. HEDGING WEATHER RISKS

A hedging example is considered in this section, in which the insurer's weather exposures are hedged with index-based instruments. The purpose of this example is two-fold. First, by applying the statistical model proposed in Section 3, the LSHAC dependence assumption is assessed for improvements in weather risk hedging through reducing basis risk. Second, four hedging strategies are developed to investigate the impact of geographical aggregation levels on the effectiveness of the weather hedge. It should be pointed out that in our analysis of the hedging effectiveness, we do not take into consideration the parameter uncertainty. The estimated parameters from Section 3 are assumed to be the true parameters when assessing the effectiveness of the various strategies for hedging weather risk. The issue with the parameter uncertainty can be addressed via methods such as bootstrapping or Bayesian analysis.

A financial weather contract is a weather contingent contract that pays claims based on future realization of weather events determined from certain weather indices. It can take the form of either a WD or a weather index-based insurance (WIBI) product. Both WD's and WIBI products are triggered by the outcome of the underlying weather index. The differences between WD and WIBI are primarily a concern for regulators and policymakers (Dischel and Barrieu, 2002). Therefore, in this example, we do not identify the differences between the two (such as using the same pricing methodology) unless necessary and collectively refer to both as WDs.

Indices based on temperature have been shown to exhibit strong correlation with crop yield (Parodi, 2014), and temperature-based derivatives have been shown to be effective at hedging weather risks that are traded on the CME (Woodard and Garcia, 2008a,b). It follows, therefore, that temperature indices could serve as feasible proxies to assess the weather risk exposure of the insurance company. The most popular weather index, heating degree days (HDD), is defined as the difference between the DAT and the base temperature ($\widetilde{T}$) if DAT falls below $\widetilde{T}$; otherwise, its value is zero. Other popular temperature indices include Cooling Degree Days (CDD) and Cumulative Average Temperature (CAT). CDD is set to zero if the DAT is smaller than $\widetilde{T}$; otherwise, it is the difference between the DAT and the base temperature $\widetilde{T}$. CAT is calculated by summing DAT over the contract period. In this paper, we focus on WDs that are based on HDD.

The setup of our numerical experiment is as follows. Let us first focus on the insurer's exposure to weather risks. The farmers are interested in insuring against their crop yield losses by purchasing weather-based (insurance) contracts (i.e. WIBI) from the insurer. We assume the insurer is a nationwide company that has underwritten a representative WIBI to each of the eight provinces in Canada. The WIBI for each province i is based on seasonal accumulated HDD (AccHDD) over the growing season (May–October). The payout of WIBI is given by $(P_i - K_i)_+ = \max(0, P_i - K_i)$, where P_i is the AccHDD in province i and K_i is a pre-determined constant. By denoting $[t_1, t_2]$ as the range of the

Downloaded from https://www.cambridge.org/core. NTU Library, on 08 Jan 2020 at 04:20:35, subject to the Cambridge Core terms of use, available at https://www.cambridge.org/core/terms. https://doi.org/10.1017/asb.2018.6

growing season, then

$$P_i = \sum_{t=t_1}^{t_2} \mathrm{HDD}_t. \tag{9}$$

This implies that the total risk exposure of the insurer is given by the portfolio of WIBI underwritten to the eight provinces, thus highlighting the importance of spatial dependence of the weather risks. By denoting X^{Exp} as the total risk exposure random variable of the insurer, then we have

$$X^{\mathrm{Exp}} = c \sum_{i=1}^{8} (P_i - K_i)_+, \tag{10}$$

where c is a proportional constant so as the risk exposure is modelled according to a portfolio totalling \$1,000 million. This is consistent with the agriculture insurance premium in Canada of \$1,090 million in 2008 (Mahul and Stutley, 2010; Agriculture and Agri-Food Canada (AAFC), 2012).

4.1. Hedging strategies

In practice, there exists a number of ways that can be used by the insurer to hedge its total weather risk exposure X^{Exp}. A most direct approach is through reinsurance. Another possible solution is via the capital market which is our main interest. In particular, we assume that the hedging instrument adopted by the insurer is the WD. Because WD is traded over-the-counter, the insurer has the flexibility of designing a WD with any appropriate payoff structure. Given this flexibility, we develop four hedging strategies, with various levels of geographical aggregation, and assess their relative effectiveness.

Additional assumptions on our proposed hedging strategies are as follows:

- Only non-linear hedging strategies involving WDs with payout resembling a call option are considered.
- The prices of the of WDs (and WIBI) are calculated under $\mathbb{Q}$ measure with Esscher transform, while the hedging performances are examined under $\mathbb{P}$ measure.
- The hedging strategy is developed based on a budget constraint, such that the price of the hedging portfolio is no more than the total premium received from underwriting WIBI.
- Our objective is to find an appropriate hedging portfolio X^{Hedge} involving WDs that minimizes the volatility of the insurer's resulting risk exposure.
- The hedging portfolio can be any subset of $\mathcal{B}$ where

$$\mathcal{B} = \Big\{\mathrm{AB}, \mathrm{SK}, \mathrm{BC}, \mathrm{MB}, \mathrm{ON}, \mathrm{NB}, \mathrm{NS}, \mathrm{QC}\Big\}.$$

Downloaded from https://www.cambridge.org/core. NTU Library, on 08 Jan 2020 at 04:20:35, subject to the Cambridge Core terms of use, available at https://www.cambridge.org/core/terms. https://doi.org/10.1017/asb.2018.6

More specifically, the insurer could use a WD with payout that depends on the weather index of any individual province or weather indices of any combination of provinces. The insurer could also use a few WDs, not just a single WD to hedge its weather risk. Without any prior information, the insurer has 2^8 choices to construct the hedging portfolio. The hierarchical structure corresponds to the LSHAC, on the other hand, provides valuable information on the spatial dependence of the weather risks, and this information can be exploited in the design of the hedging strategy.

We now describe the four hedging strategies:

Strategy 1: *Local hedging strategy*

By local hedging, we mean that the insurer hedges its weather risks by only resorting to a WD with payout based on a single province. Suppose $X_{1,g}^{\text{Hedge}}$, $g \in \mathcal{B}$ denotes the hedging instrument adopted by the insurer. We assume that the payout of the hedging instrument is given by

$$X_{1,g}^{\text{Hedge}} = \gamma_g (P_g - K_g)_+, \tag{11}$$

where γ_g can be interpreted as the face value (or the number of units) of the WD. Let $X_{1,g}^{\text{HP}}$ be the hedged portfolio, i.e. the value of the portfolio after hedging. Then we have

$$X_{1,g}^{\text{HP}} = X_{1,g}^{\text{Hedge}} - X^{\text{Exp}} + E^{\mathbb{Q}}(X^{\text{Exp}}) - E^{\mathbb{Q}}\left(X_{1,g}^{\text{Hedge}}\right). \tag{12}$$

The optimal value of γ_g is determined as the solution to the following variance minimization problem:

$$\min_{\gamma_g} \sqrt{\text{Var}^{\mathbb{P}}\left(X_{1,g}^{\text{HP}}\right)},$$

$$\text{subject to } \; E^{\mathbb{Q}}(X_{1,g}^{\text{Hedge}}) \leq E^{\mathbb{Q}}\left(X^{\text{Exp}}\right). \tag{13}$$

In addition to the local hedging, we also consider more complicated strategies that reflect the spatial structure of the weather risks. We refer these strategies as "global hedging strategies". In theory, the higher the geographical aggregation level of the hedge, the more offsetting of risks in the portfolio (i.e. natural diversification). Therefore, the risk that is remaining is more systematic in nature and may be better suited for hedging. Therefore, global hedging strategies with different levels of spatial aggregation in the hedging portfolios are proposed to investigate the geographical aggregation effect.

Strategy 2: *Three parts global hedging strategy*

This strategy exploits the hierarchical structure of Figure 3 by considering a hedging portfolio that comprises of three parts. Let X_2^{Hedge} denote the hedging portfolio, then

$$X_2^{\text{Hedge}} = X_{2,g_{2,1}}^{\text{Hedge}} + X_{2,g_{2,2}}^{\text{Hedge}} + X_{2,g_{2,3}}^{\text{Hedge}},$$

Downloaded from https://www.cambridge.org/core. NTU Library, on 08 Jan 2020 at 04:20:35, subject to the Cambridge Core terms of use, available at https://www.cambridge.org/core/terms. https://doi.org/10.1017/asb.2018.6

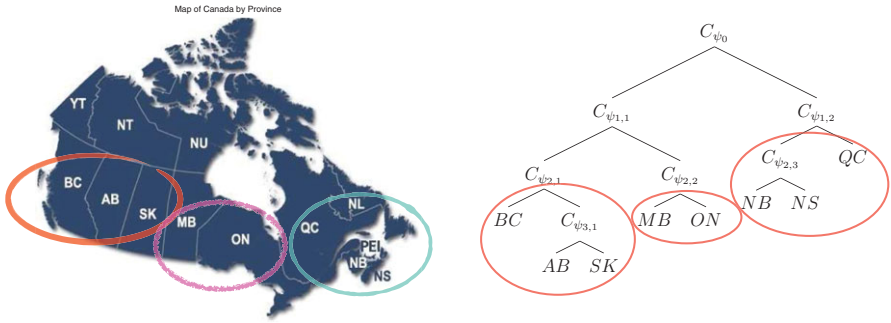


FIGURE 4: Illustration of the three parts global hedging strategy, where the eight provinces are partitioned into three groups based on the hierarchical structure of Figure 3 and neighbouring provinces are put into the same hedging portfolios. (Color online)

where

$$X^{\text{Hedge}}_{2,g_{2,j}} = \left(\sum_{g_j \in g_{2,j}} \omega_{g_j} P_{g_j} - \sum_{g_j \in g_{2,j}} \delta_{g_j} K_{g_j} \right)_+, \quad j = 1, 2, 3.$$

Here, $g_{2,1} = \{\text{AB, SK, BC}\}$, $g_{2,2} = \{\text{MB, ON}\}$, $g_{2,3} = \{\text{NB, NS, QC}\}$ and δ_{g_j} is defined to reflect the number of regions (i.e. provinces) in each group:

$$\delta_{g_j} = \begin{cases} \frac{1}{3} & j = 1 \text{ or } 3, \\ \frac{1}{2} & j = 2. \end{cases}$$

Figure 4 displays the geographical location of these partitions and also demonstrates how these partitions relate to the hierarchical structure of the LSHAC.

Hence, the corresponding hedged portfolio is $X_2^{\text{HP}} = X_2^{\text{Hedge}} - X^{\text{Exp}} + E^{\mathbb{Q}}(X^{\text{Exp}}) - E^{\mathbb{Q}}(X_2^{\text{Hedge}})$. For the above hedging strategy, the parameters ω_{g_j}, $j = 1, 2, 3$ have yet to be specified. These parameters can be obtained optimally by solving the following optimization problem:

$$\min_{\omega_{g_j}, j=1,2,3} \sqrt{\text{Var}^{\mathbb{P}}(X_2^{\text{HP}})},$$

$$\text{subject to} \quad E^{\mathbb{Q}}(X_2^{\text{Hedge}}) \leq E^{\mathbb{Q}}(X^{\text{Exp}}),$$

$$\sum_{j=1}^{3} \sum_{g_j \in g_{2,j}} \omega_{g_j} = 1.$$

Strategy 3: *Two parts global hedging strategy*

The two parts global hedging strategy increases the geographical aggregation level by partitioning the eight provinces into two parts based on the hierarchi-

Downloaded from https://www.cambridge.org/core. NTU Library, on 08 Jan 2020 at 04:20:35, subject to the Cambridge Core terms of use, available at https://www.cambridge.org/core/terms. https://doi.org/10.1017/asb.2018.6

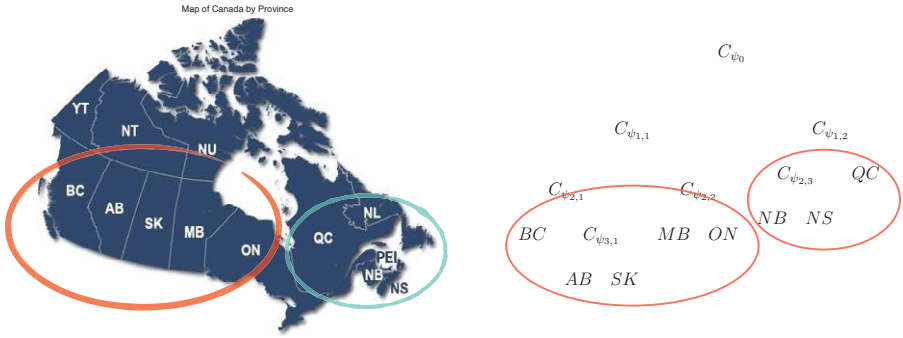


FIGURE 5: Illustration of the two parts global hedging strategy, where the eight provinces are partitioned into two groups based on the hierarchical structure of Figure 3, and neighbour provinces are put into the same hedging portfolios. (Color online)

cal structure in Figure 3. Analogously denoting X_3^{Hedge} as the corresponding hedging portfolio, we have

$$X_3^{\text{Hedge}} = X_{3,g_{3,1}}^{\text{Hedge}} + X_{3,g_{3,2}}^{\text{Hedge}},$$

where

$$X_{3,g_{3,k}}^{\text{Hedge}} = \left(\sum_{g_k \in g_{3,k}} \omega_{g_k} P_{g_k} - \sum_{g_k \in g_{3,k}} \delta_{g_k} K_{g_k} \right)_+, \quad k = 1, 2,$$

$g_{3,1} = \{\text{AB, SK, BC, MB, ON}\}$, $g_{3,2} = \{\text{NB, NS, QC}\}$, and δ_{g_k} is defined as

$$\delta_{g_k} = \begin{cases} \frac{1}{5} & j = 1, \\ \frac{1}{3} & j = 2. \end{cases}$$

Similarly, Figure 5 provides a graphical representation of the partition and their relationship to the hierarchical structure of the LSHAC.

As in the previous strategy, the resulting hedged portfolio becomes $X_3^{\text{HP}} = X_3^{\text{Hedge}} - X^{\text{Exp}} + E^{\mathbb{Q}}(X^{\text{Exp}}) - E^{\mathbb{Q}}(X_3^{\text{Hedge}})$ so that the corresponding optimization problem becomes

$$\min_{\omega_{g_k}, k=1,2} \sqrt{\text{Var}^{\mathbb{P}}(X_3^{\text{HP}})},$$

$$\text{subject to} \quad E^{\mathbb{Q}}(X_3^{\text{Hedge}}) \leq E^{\mathbb{Q}}(X^{\text{Exp}}),$$

$$\sum_{k=1}^{2} \sum_{g_k \in g_{3,k}} \omega_{g_k} = 1.$$

Strategy 4: *One part global hedging strategy*

Downloaded from https://www.cambridge.org/core. NTU Library, on 08 Jan 2020 at 04:20:35, subject to the Cambridge Core terms of use, available at https://www.cambridge.org/core/terms. https://doi.org/10.1017/asb.2018.6

The final one part global hedging strategy aggregates all eight provinces into a single hedging portfolio. Therefore, this hedging strategy has the highest geographical aggregation level, which may have the most natural diversification effect. Let X_4^{Hedge} represent the hedging portfolio, then

$$X_4^{\text{Hedge}} = \left(\sum_{g \in \mathcal{B}} \omega_g P_g - \sum_{g \in \mathcal{B}} \delta_g K_g \right)_+,$$

where $\delta_g = 1/8$. The hedged portfolio is similarly given by $X_4^{\text{HP}} = X_4^{\text{Hedge}} - X^{\text{Exp}} + E^{\mathbb{Q}}(X^{\text{Exp}}) - E^{\mathbb{Q}}(X_4^{\text{Hedge}})$, and thus the optimization problem is formulated as

$$\min_{\omega_g, g \in \mathcal{B}} \sqrt{\text{Var}^{\mathbb{P}}(X_4^{\text{HP}})},$$

$$\text{subject to} \quad E^{\mathbb{Q}}(X_4^{\text{Hedge}}) \leq E^{\mathbb{Q}}(X^{\text{Exp}}),$$
$$\sum_{g \in \mathcal{B}} \omega_g = 1.$$

4.2. Hedging effectiveness

In this section, the results of the different hedging strategies are discussed. To assess the effectiveness of each hedging strategy, there are several problems that are of interest, including (1) the implication of a hedged vs. unhedged portfolio (i.e. the necessity of hedging weather risk); (2) the importance of the assumed underlying dependence structure; (3) the geographical aggregation effect on hedging effectiveness. First, we gauge the effectiveness of the various hedging strategies using the following three criteria:

1. *Weather risk variance reduction:* Following Li and Hardy (2011), we define the hedging efficiency of hedging strategy j, denoted by Ef_j in term of its effect on risk reduction. More specifically, this is defined as

$$Ef_j = 1 - \frac{\text{Var}^{\mathbb{P}}(X_j^{\text{HP}})}{\text{Var}^{\mathbb{P}}(X^{\text{Exp}})}, \quad j = 1, \ldots, 4, \tag{14}$$

   so that Ef_j is bounded between 0 and 1. If Ef_j is close to one, then the hedging portfolio is an efficient strategy in the sense that it is extremely effective at reducing the volatility of the insurer's risk exposure. On the other hand, a small value of Ef_j signifies inefficiency of the hedging portfolio. In the extreme case with $Ef_j = 0$, then the hedging portfolio has no impact on the risk exposure of the insurer. This is equivalent to the "naked" position of the insurer in that the insurer does not hedge.

Downloaded from https://www.cambridge.org/core. NTU Library, on 08 Jan 2020 at 04:20:35, subject to the Cambridge Core terms of use, available at https://www.cambridge.org/core/terms. https://doi.org/10.1017/asb.2018.6

2. *Weather risk value-at-risk (VaR):* For each hedged portfolio, X_*^{HP}, we calculate its VaR at the 1% level, defined as $\mathrm{VaR}_{0.01} = F^{-1}_{X_*^{\mathrm{HP}}}(0.01)$, where the subscript "*" denotes a certain hedging strategy. As the 1% quantile of the hedged portfolio, $\mathrm{VaR}_{0.01}$ characterizes the left tail of the hedged portfolio distribution. Therefore, a high value of $\mathrm{VaR}_{0.01}$ indicates a better hedging strategy. To compare the hedging effectiveness, we also calculate the $\mathrm{VaR}_{0.01}$ of the unhedged portfolio.
3. *Weather risk conditional tail expectation (CTE):* The 1% level CTE, also called Expected Shortfall, of a random variable X, defined as $\mathrm{CTE}_{0.01} = E(X|X < \mathrm{VaR}_{0.01})$, calculates the average losses that have exceeded $\mathrm{VaR}_{0.01}$, providing more information about the extreme scenarios. As a result, CTE is sometimes preferred by risk managers in practice (Acerbi and Tasche, 2002). Therefore, we calculate and compare the $\mathrm{CTE}_{0.01}$ of each hedged (and unhedged) portfolio to see the hedging effectiveness.

The first criterion measures the weather hedging efficiency in terms of the variance reduction effect, while the second and the third focus on the reduction in the downside risk, i.e., the worst-case scenario of the portfolio. We use the CL assumption as a benchmark model since it performs better than the GM (see Table 7). We discuss the hedging results of each strategy with different MPR parameters (Turvey, 2005) by assuming θ to be $\{0, 0.1, 0.3, 0.5\}$. The results of the different hedging strategies are displayed in Tables 8, 9, and Figures 6 and 7.

Necessity of hedging weather risk

An efficient hedging strategy should achieve a large reduction in risk, and help the insurance company maintain stable future cash flows. Table 8 displays the hedging efficiencies of different hedging strategies. It is obvious that all strategies are able to reduce the portfolio risks significantly under both dependence structure assumptions, since they have reduced the dispersion of the portfolios. The best hedge, i.e., three-part global hedge, has hedging efficiency of more than 95% for both dependence structure assumptions and all MPR assumptions. In fact, even the hedge with the worst performance, i.e., the local-SK strategy, it can still reduce the variance by at least 43%. The relative performances of the local hedging strategy, global hedging strategy, as well as the unhedged position, are highlighted and contrasted in both Figures 6 and 7. In these two figures, the simulated distributions of unexpected cash flows for different hedging strategies (MPR assumption: $\theta = 0$) are plotted based on the CL assumption and the LSHAC copula assumption, respectively.

Importance of dependence structures

It is important to understand the impact of introducing the dependence structure in the statistical modelling of temperature with respect to improving hedging performance. In particular, under all MPR assumptions the LSHAC model has better hedging performance compared to the CL assumption. Table 8 shows that under each MPR assumption, the LSHAC models achieve higher

Downloaded from https://www.cambridge.org/core. NTU Library, on 08 Jan 2020 at 04:20:35, subject to the Cambridge Core terms of use, available at https://www.cambridge.org/core/terms. https://doi.org/10.1017/asb.2018.6

TABLE 8

HEDGING EFFICIENCIES OF FOUR STRATEGIES.

		ton				C			
		$\theta = 0$	$\theta = 0.1$	$\theta = 0.3$	$\theta = 0.5$	$\theta = 0$	$\theta = 0.1$	$\theta = 0.3$	$\theta = 0.5$
Local	AB	0.4668	0.4668	0.4668	0.4668	0.4961	0.4961	0.4961	0.4961
	BC	0.7147	0.7147	0.7147	0.7147	0.7335	0.7335	0.7335	0.7335
	MB	0.7442	0.7442	0.7442	0.7442	0.7371	0.7371	0.7371	0.7371
	NB	0.8454	0.8454	0.8454	0.8454	0.8533	0.8533	0.8533	0.8533
	NS	0.8461	0.8461	0.8461	0.8461	0.8441	0.8441	0.8441	0.8441
	ON	0.7865	0.7865	0.7865	0.7865	0.7288	0.7288	0.7288	0.7288
	QC	0.6148	0.6148	0.6148	0.6148	0.5140	0.5140	0.5140	0.5140
	SK	0.4319	0.4319	0.4319	0.4319	0.4390	0.4390	0.4390	0.4390
Global	Three parts	0.9761	0.9771	0.9584	0.9123	0.9836	0.9819	0.9599	0.9767
	Two parts	0.9286	0.9286	0.9280	0.9154	0.9151	0.9151	0.9121	0.9029
	One part	0.9101	0.9101	0.9101	0.9101	0.9128	0.9128	0.9128	0.9128

Local hedging strategies have eight choices, i.e. the insurance company can select the HDD from eight provinces to hedge the weather risks. Clayton and LSHAC copula assumptions are compared. In addition, results for different MPR assumptions are displayed.

Downloaded from https://www.cambridge.org/core. NTU Library, on 08 Jan 2020 at 04:20:35, subject to the Cambridge Core terms of use, available at https://www.cambridge.org/core/terms. https://doi.org/10.1017/asb.2018.6

TABLE 9

$VaR_{0.01}$ AND $CTE_{0.01}$ OF SIMULATED DISTRIBUTIONS OF UNEXPECTED CASH FLOWS FOR FOUR STRATEGIES.

			Clayton				LSHAC			
			$\theta = 0$	$\theta = 0.1$	$\theta = 0.3$	$\theta = 0.5$	$\theta = 0$	$\theta = 0.1$	$\theta = 0.3$	$\theta = 0.5$
Local	AB	VaR	−215.76	−253.21	−263.73	−70.24	−215.91	−251.97	−237.88	−68.90
		CTE	−232.09	−269.54	−280.05	−86.56	−231.26	−267.32	−253.22	−84.25
	BC	VaR	−117.73	−107.28	−106.20	−136.61	−116.59	−104.56	−104.71	−135.42
		CTE	−123.43	−112.98	−111.90	−142.31	−121.85	−109.82	−109.97	−140.68
	MB	VaR	−57.91	−81.54	−158.66	−207.92	−58.20	−81.55	−160.38	−208.96
		CTE	−63.72	−87.36	−164.47	−213.74	−63.87	−87.21	−166.04	−214.63
	NB	VaR	−73.63	−69.75	−120.09	−168.22	−73.34	−68.97	−120.41	−167.94
		CTE	−79.74	−75.86	−126.19	−174.33	−79.62	−75.25	−126.68	−174.22
	NS	VaR	−57.17	−70.97	−138.96	−187.84	−57.14	−71.17	−139.67	−188.25
		CTE	−63.23	−77.03	−145.02	−193.90	−62.88	−76.91	−145.41	−193.99
	ON	VaR	−104.99	−92.35	−99.77	−139.52	−110.24	−101.87	−110.70	−142.12
		CTE	−110.35	−97.72	−105.14	−144.89	−115.38	−107.02	−115.85	−147.27
	QC	VaR	−200.06	−249.49	−288.34	−63.56	−211.44	−265.68	−354.64	−73.14
		CTE	−216.28	−265.72	−304.57	−79.79	−226.53	−280.77	−369.73	−88.23
	SK	VaR	−150.37	−150.37	−150.37	−130.28	−150.88	−150.88	−150.88	−130.80
		CTE	−155.99	−155.99	−155.99	−135.90	−155.86	−155.86	−155.86	−135.79
Global	Three parts	VaR	−15.49	−17.29	−47.52	−39.48	−13.50	−18.84	−46.36	−9.54
		CTE	−20.00	−22.65	−52.39	−42.88	−18.53	−24.01	−49.80	−16.30
	Two parts	VaR	−20.95	−26.48	−94.60	−147.23	−22.86	−30.78	−103.78	−155.46
		CTE	−23.73	−29.25	−97.39	−149.73	−25.51	−33.42	−106.30	−157.88
	One part	VaR	−25.21	−34.18	−108.79	−158.04	−25.14	−33.73	−108.80	−157.36
		CTE	−28.38	−37.34	−111.96	−161.20	−28.47	−37.06	−112.13	−160.69

Local hedging strategies have eight choices, i.e. the insurance company can select the HDD from eight provinces to hedge the weather risks. The Clayton copula and LSHAC dependent structure assumptions are compared. In addition, results for different MPR assumptions are displayed. (million $)

Downloaded from https://www.cambridge.org/core. NTU Library, on 08 Jan 2020 at 04:20:35, subject to the Cambridge Core terms of use, available at https://www.cambridge.org/core/terms. https://doi.org/10.1017/asb.2018.6

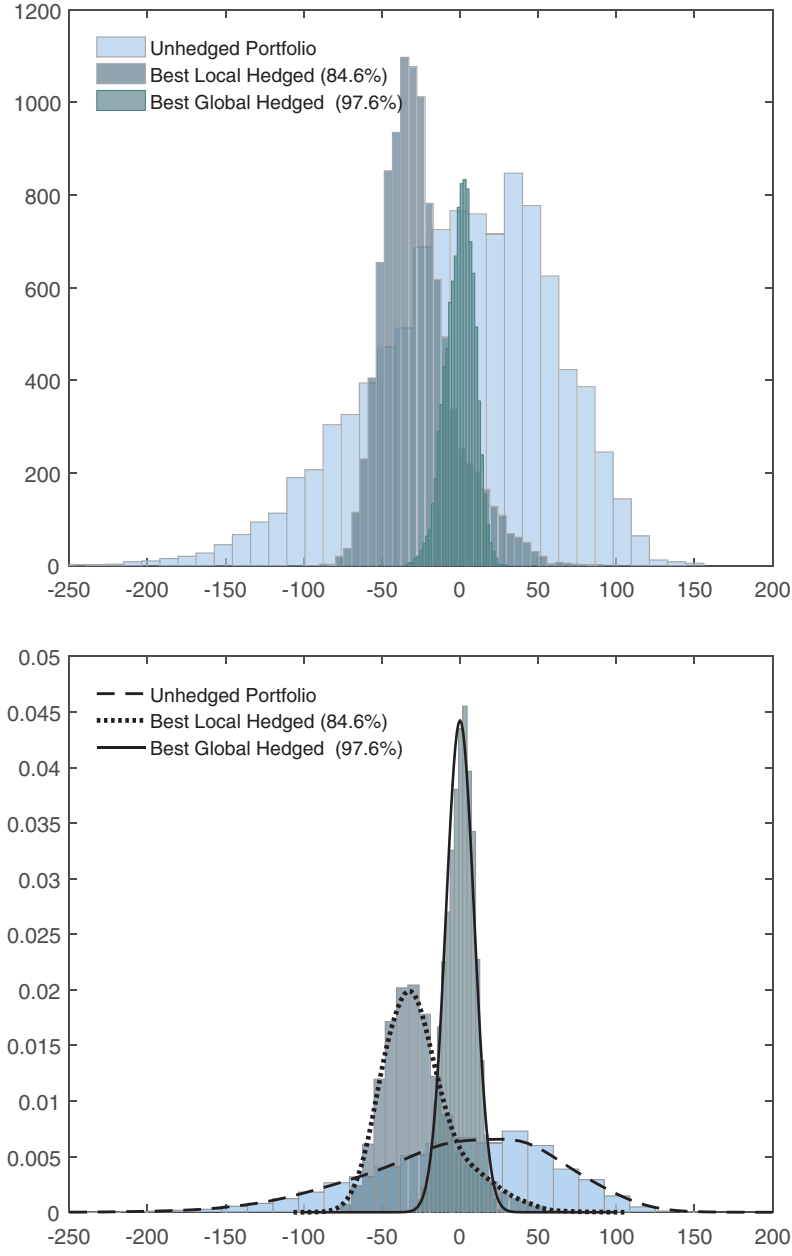


FIGURE 6: Simulated distributions of unexpected cash flows for different hedging strategies based on the Clayton copula assumption (MPR assumption: $\theta = 0$). The first figure shows the actual counting frequencies, and the second figure shows the normalized frequencies with fitted kernel density curves. The dashed line is for the unhedged portfolio, the dotted line is for the best local hedging strategy and the solid line is for the best global hedging strategy. (Color online)

Downloaded from https://www.cambridge.org/core. NTU Library, on 08 Jan 2020 at 04:20:35, subject to the Cambridge Core terms of use, available at https://www.cambridge.org/core/terms. https://doi.org/10.1017/asb.2018.6

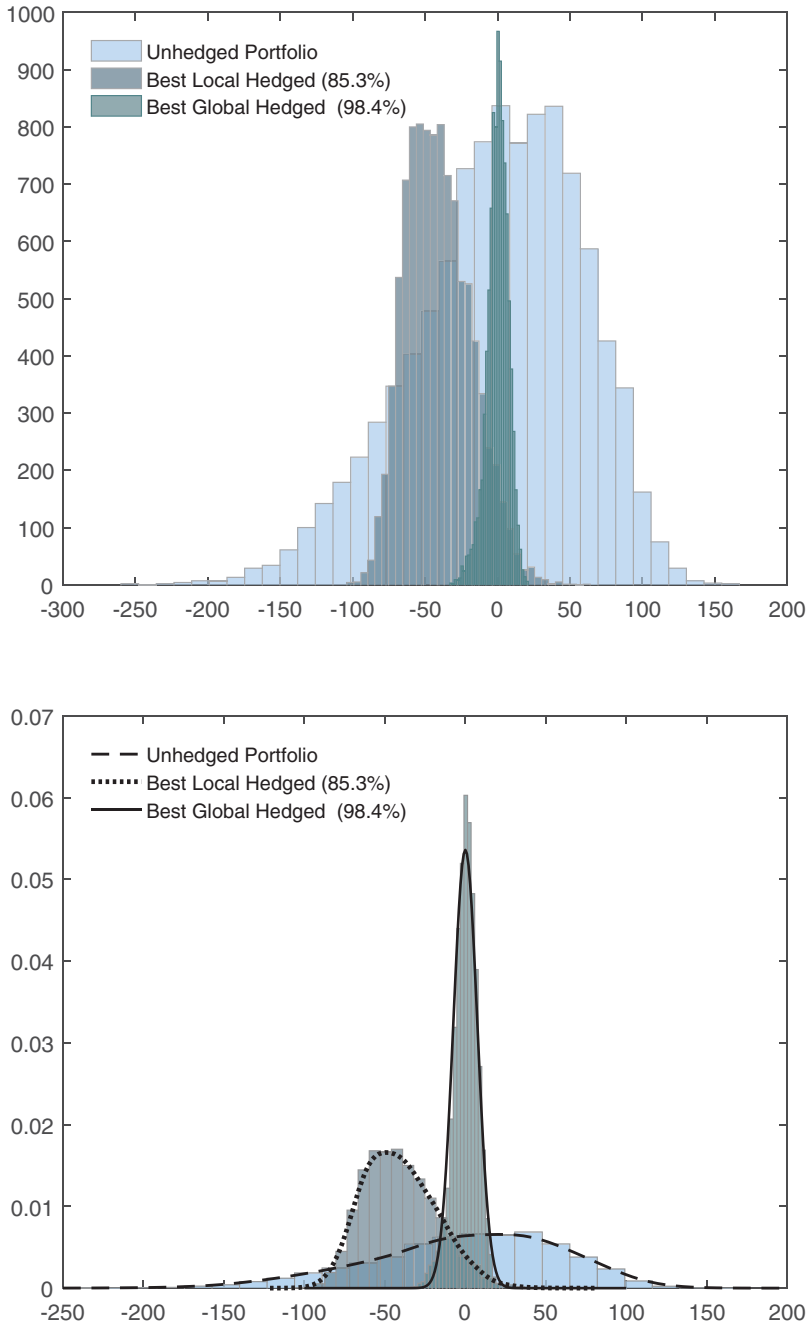


FIGURE 7: Simulated distributions of unexpected cash flows for different hedging strategies based on the LSHAC copula assumption (MPR assumption: $\theta = 0$). The first figure shows the actual counting frequencies, and the second figure shows the normalized frequencies with fitted kernel density curves. The dashed line is for the unhedged portfolio, the dotted line is for the best local hedging strategy and the solid line is for the best global hedging strategy. (Color online)

Downloaded from https://www.cambridge.org/core. NTU Library, on 08 Jan 2020 at 04:20:35, subject to the Cambridge Core terms of use, available at https://www.cambridge.org/core/terms. https://doi.org/10.1017/asb.2018.6

hedging efficiencies relative to the CL assumption. In addition, the LSHAC model in general can reduce the downside risk of the portfolio further than the CL, which is shown in Table 9.

Geographical aggregation effect

The empirical results imply that hedging strategies with higher geographical aggregation levels are more effective. More specifically, we find that hedging strategies with higher levels of aggregation have superior performance in hedging systematic weather risk. It is interesting to note that the local hedging strategy has the lowest level of geographical aggregation among all hedging strategies, and also has the worst performance compared to the global hedging strategies, while global hedging strategies are more effective. These results are consistent with previous work by Woodard and Garcia (2008a,b), which showed that agricultural hedging can be improved as the spatial aggregation of the risk exposure and hedging instrument increases.

5. Concluding remarks

Adverse weather is a main source of crop production loss and a large concern for agricultural insurers and reinsurers. A main source of agricultural insurance market failure has been attributed to the systemic nature of weather risks (Miranda and Glauber, 1997; Woodard and Garcia, 2008b), which can be widespread and spatially correlated at times. Therefore, weather risks cannot be diversified by pooling alone, and various risk transfer techniques must be considered. In response, weather risk hedging through WDs or WIBI products may be valuable. However, due to basis risk weather risk hedging has been largely unsuccessful to date.

In this paper, we study the systemic weather risk in Canada and develop different weather risk hedging strategies that may be considered by agricultural insurers and reinsurers. In developing the weather risk hedging strategies, the statistical modelling of weather variables was refined. This is an essential, yet, challenging task for financial weather instrument pricing and hedging, owing to the non-stationarity, seasonality and multidimensionality of the weather data, as well as the incomplete nature of the market. In this paper, Fourier series was used to capture the seasonalities in both the original temperature series as well as in the volatilities of the data, in addition to the EGARCH(1,1) process. To overcome the high-dimensionality of the weather data and model the spatial dependence of weather events in order to reduce basis risk and improve the efficiency of weather hedging, this paper proposed a new copula family called the LSHAC model. This was the first paper to employ the LSHAC for modelling the geographical dependence of weather events. Finally, a pricing framework was proposed based on the conditional Esscher transform method to address the challenge of instrument pricing in an incomplete market, which has also contributed to the unsuccessful implementation of weather risk hedging in addition to basis risk.

Downloaded from https://www.cambridge.org/core. NTU Library, on 08 Jan 2020 at 04:20:35, subject to the Cambridge Core terms of use, available at https://www.cambridge.org/core/terms. https://doi.org/10.1017/asb.2018.6

To examine the modelling framework proposed in this paper, an empirical analysis was conducted using 50 years of temperature data corresponding to eight provinces in Canada. Using the refined statistical modelling of the weather data proposed in this paper, four weather hedging strategies were developed and compared. In assessing the effectiveness of the various hedging strategies, three problems were considered: (1) the necessity of hedging weather risk; (2) the importance of the assumed underlying dependence structure; and (3) the geographical aggregation effect on hedging effectiveness. The results lend support to the importance of capturing the appropriate dependence structure of weather risk, which leads to more efficient hedging strategies. Moreover, the analysis shows that the LSHAC model can improve the hedging performance through more accurate modelling of the dependence structure of weather risks and is more efficient in hedging extreme downside weather risk, compared to the benchmark copula models. Further, the results reveal that more effective hedging may be achieved as the spatial aggregation level increases. This research demonstrates that hedging weather risk is an important risk management method, and the approach outlined in this paper may be useful to insurers and reinsurers in the case of agriculture, as well as for other related risk in the property and casualty sector.

Acknowledgements

Zhu acknowledges the research funding support from the Nanyang Technological University Start Up Grant (M4082106.010). Porth and Tan acknowledge the research funding from Social Sciences and Humanities Research Council (SSHRC). Wang acknowledges the research funding support from the Ministry of Science and Technology (105-2410-H-110 -089 -MY2).

Notes

1. One limitation of the two-stage estimation procedure is that the second-stage estimation tends to underestimate the standard errors. Therefore, in the empirical results in Section 3.2, only standard errors (instead of t-statistics tests) from the second-stage estimation are displayed, because in the two-stage estimation procedure, showing t-statistics of the second stage is not useful.

2. To save space, the estimation results of the 25 cyclical lags ($\rho_{l,i}; l = 1, \ldots, L, i = 1, \ldots, d$) are not included but are available upon request. It is shown from the estimated results for cyclical lags that although, for some provinces (AB and ON), higher order autoregressive coefficients are necessary, for most of the cases, using three to four lags are sufficient to capture the long memory of the temperature data.

3. For a detailed introduction of hierarchical clustering analysis, refer to Ward (1963), Székely and Rizzo (2005) and Zhang *et al.* (2013). For detailed algorithms of grouping method for the LSHAC, refer to Zhu *et al.* (2016).

4. To improve computational efficiency, we use the most recent 10 years of the pseudo samples to estimate the dependence structure.

References

Abdallah, A., Boucher, J.-P. and Cossette, H. (2015) Modeling dependence between loss triangles with hierarchical archimedean copulas. *ASTIN Bulletin: A Journal of the IAA,* **45**(3), 577–599.

Downloaded from https://www.cambridge.org/core. NTU Library, on 08 Jan 2020 at 04:20:35, subject to the Cambridge Core terms of use, available at https://www.cambridge.org/core/terms. https://doi.org/10.1017/asb.2018.6

ACERBI, C. and TASCHE, D. (2002) Expected shortfall: A natural coherent alternative to value at risk. *Economic Notes*, **31**(2), 379–388.

Agriculture and Agri-Food Canada (AAFC) (2012) *Evaluation of the Agriinsurance, Private Sector Risk Management Partnerships and Wildlife Compensation Programs*. Technical Report AAFC No. 11985E, Agriculture and Agri-Food Canada, Office of Audit and Evaluation.

ALEXANDRIDIS, A.K. and ZAPRANIS, A.D. (2013) *Weather Derivatives, Modeling and Pricing Weather-Related Risk*. USA: Springer.

ARBENZ, P. and CANESTRARO, D. (2012) Estimating copulas for insurance from scarce observations, expert opinion and prior information: A bayesian approach. *ASTIN Bulletin: A Journal of the IAA*, **42**(1), 271–290.

AVANZI, B., CASSAR, L.C. and WONG, B. (2011) Modelling dependence in insurance claims processes with lévy copulas. *ASTIN Bulletin: A Journal of the IAA*, **41**(2), 575–609.

BARTH, A., BENTH, F.E. and POTTHOFF, J. (2011) Hedging of spatial temperature risk with market-traded futures. *Applied Mathematical Finance*, **18**(2), 93–117.

BENTH, F.E. and BENTH, J.Š. (2013) *Modeling and Pricing in Financial Markets for Weather Derivatives*. Singapore: World Scientific.

BÜHLMANN, H., DELBAEN, F., EMBRECHTS, P. and SHIRYAEV, A.N. (1996) No-arbitrage, change of measure and conditional Esscher transforms. *CWI Quarterly*, **9**(4), 291–317.

CAMPBELL, S.D. and DIEBOLD, F.X. (2005) Weather forecasting for weather derivatives. *Journal of the American Statistical Association*, **100**(469), 6–16.

CARRIQUIRY, M.A. and OSGOOD, D.E. (2012) Index insurance, probabilistic climate forecasts, and production. *Journal of Risk and Insurance*, **79**(1), 287–300.

CHULIÁ, H., GUILLÉN, M. and URIBE, J.M. (2016) Modeling longevity risk with generalized dynamic factor models and vine-copulae. *ASTIN Bulletin: A Journal of the IAA*, **46**(1), 165–190.

COBLE, K., KNIGHT, T., MILLER, M., GOODWIN, B., REJESUS, R. and BOYLES, R. (2013) Estimating structural change in u.s. crop insurance experience. *Agricultural Finance Review*, **73**(1), 74–87.

COBLE, K.H., MILLER, M.F., REJESUS, R.M., BOYLES, R., KNIGHT, T.O. and GOODWIN, B.K. (2011) *Methodology Analysis for Weighting of Historical Experience*. USDA Risk Management Agency.

CUMMINS, J.D., LALONDE, D. and PHILLIPS, R.D. (2004) The basis risk of catastrophic-loss index securities. *Journal of Financial Economics*, **71**, 77–111.

DISCHEL, R.S. and BARRIEU, P. (2002) Financial weather contracts and their application in risk management. In *Climate Risk and the Weather Market: Financial Risk Management With Weather Hedges* (ed. R.S. Dischel), pp 25–42. London, UK: Risk Books.

DONG, W., SHAH, H. and WONG, F. (1996) A rational approach to pricing of catastrophe. *Journal of Risk and Uncertainty*, 12(2–3):201–218.

DUPUIS, D.J. (2012) Modeling waves of extremes temperature: The changing tails of four cities. *Journal of the American Statistical Association*, **107**(497), 24–39.

DUPUIS, D.J. (2014) A model for nighttime minimum temperatures. *Journal of Climate*, **27**(19), 7207–7229.

EMBRECHTS, P. and HOFERT, M. (2013) Statistical inference for copulas in high dimensions: A simulation study. *ASTIN Bulletin: A Journal of the IAA*, **43**(2), 81–95.

EMBRECHTS, P., LINDSKOG, F. and MCNEIL (2003) Modelling dependence with copulas and applications to risk management. *Handbook of Heavy Tailed Distributions in Finance*, **8**(1), 329–284.

ERHARDT, R.J. (2015) Incorporating spatial dependence and climate change trends for measuring long-term temperature derivative risk. *Variance*, **9**(2), 213–226.

ERHARDT, R.J. and SMITH, R.L. (2014) Weather derivative risk measures for extreme events. *North American Actuarial Journal*, **18**(3), 379–393.

FRITTELLI, M. (2000) The minimum entropy martingale measure and the valuation problem in incomplete markets. *Mathematical Finance*, **10**(1), 39–52.

GERBER, H. and SHIU, S. (1994) Option pricing by Esscher transforms. *Transaction of Society of Actuaries*, **46**, 99–140.

Downloaded from https://www.cambridge.org/core. NTU Library, on 08 Jan 2020 at 04:20:35, subject to the Cambridge Core terms of use, available at https://www.cambridge.org/core/terms. https://doi.org/10.1017/asb.2018.6

GOLDEN, L.L., WANG, M. and YANG, C. (2007) Handling weather related risks through the financial markets: Considerations of credit risk, basis risk, and hedging. *Journal of Risk and Insurance*, **74**(2), 319–346.
GOODWIN, B.K. (2001) Problems with market insurance in agriculture. *American Journal of Agriculture Economics*, **83**(3), 643–649.
GOODWIN, B.K. and HUNGERFORD, A. (2014) Copula-based models of systemic risk in U.S. agriculture: Implications for crop insurance and reinsurance contracts. *American Journal of Agriculture Economics*, **97**(3), 879–896.
HÄRDLE, W.K. and OSIPENKO, M. (2012) Spatial risk premium on weather derivatives and hedging weather exposure in electricity. *The Energy Journal*, **33**(2), 149–170.
HELLMUTH, M.E., OSGOOD, D.E., HESS, U., MOORHEAD, A. and BHOJWANI, H. (2009) *Index insurance and climate risk: Prospects for development and disaster management*. Technical Report No. 2, Climate and Society, International Research Institute for Climate and Society, New York, USA.
HERING, C., HOFERT, M., MAI, J.-F. and SCHERER, M. (2010) Constructing hierarchical archimedean copulas with lévy subordinators. *Journal of Multivariate Analysis*, **101**(6), 1428–1433.
HONG, H., LI, F.W. and XU, J. (2016) *Climate Risks and Market Efficiency*. Columbia University, Working Paper.
HUBALEK, J. and NEILSEN, B. (2006) On the Esscher transform and entropy for exponential Lévy models. *Quantitative Finance*, **6**(2), 125–145.
HÜRLIMANN, W. (2014) On some properties of two vector-valued VaR and CTE multivariate risk measures for Archimedean copulas. *ASTIN Bulletin: A Journal of the IAA*, **44**(3), 613–633.
IPCC (2007) *Fourth Assessment Report.* Technical report, Intergovernmental Panel on Climate Change.
JOE, H. (1997) *Multivariate Models and Dependence Concepts*. Boca Raton: Chapman & Hall.
LI, J.S.-H. and HARDY, M.R. (2011) Measuring basis risk in longevity hedges. *North American Actuarial Journal*, **15**(2), 177–200.
LI, J.S.-H., HARDY, M.R. and TAN, K.S. (2010) On pricing and hedging the no-negative-equity guarantee in equity release mechanisms. *Journal of Risk and Insurance*, **77**(2), 499–522.
LOBELL, D.B. and BURKE, M.B. (2008) Why are agricultural impacts of climate change so uncertain? The importance of temperature relative to precipitation. *Environmental Research Letters*, **3**(1), 1–8.
MAHUL, O. and STUTLEY, C.J. (2010) *Government Support to Agricultural Insurance: Challenges and Options for Developing Countries.* Washington D.C.: World Bank Publications.
MAI, J.-F. and SCHERER, M. (2012) H-extendible copulas. *Journal of Multivariate Analysis*, **110**, 151–160.
MCNEIL, A.J. (2008) Sampling nested archimedean copulas. *Journal of Statistical Computation and Simulation*, **78**(6), 567–581.
MCNEIL, A.J., FREY, R. and EMBRECHTS, P. (2010) *Quantitative Risk Management: Concepts, Techniques, and Tools*. Princeton, NJ: Princeton University Press.
MIRANDA, M. and GLAUBER, J. (1997) Systemic risk, reinsurance and the failure of crop insurance market. *American Journal of Agriculture Economics*, **79**(1), 206–215.
NELSON, D.B. (1991) Conditional heteroskedasticity in asset returns: A new approach. *Econometrica*, **59**(2), 347–370.
ODENING, M. and SHEN, Z. (2012) Challenges of insuring weather risk in agriculture. *Agricultural Finance Review*, **74**(2), 188–199.
OKHRIN, O., ODENING, M. and XU, W. (2013a) Systemic weather risk and crop insurance: The case of china. *Journal of Risk and Insurance*, **80**(2), 351–372.
OKHRIN, O., OKHRIN, Y. and SCHMID, W. (2013b) On the structure and estimation of hierarchical archimedean copulas. *Journal of Econometrics*, **173**(1), 189–204.
PARODI, P. (2014) *Pricing in General Insurance*. Boca Raton: CRC Press.
PÉREZ-GONZÁLEZ, F. and YUN, H. (2013) Risk management and firm value: Evidence from weather derivatives. *Journal of Finance*, **LXVIII**(5), 2143–2176.

Downloaded from https://www.cambridge.org/core. NTU Library, on 08 Jan 2020 at 04:20:35, subject to the Cambridge Core terms of use, available at https://www.cambridge.org/core/terms. https://doi.org/10.1017/asb.2018.6

PORTH, L., PAI, J. and BOYD, M. (2015) A portfolio optimization approach using combinatorics with a genetic algorithm for developing a reinsurance model. *Journal of Risk and Insurance*, **82**(3), 687–713.
PORTH, L., TAN, K.S. and WENG, C. (2013) Optimal reinsurance analysis from a crop insurer's perspective. *Agriculture Finance Review*, **73**(2), 310–328.
PORTH, L., ZHU, W. and TAN, K.S. (2014b) A credibility-based Erlang mixture model for pricing crop reinsurance. *Agricultural Finance Review*, **74**(2), 162–187.
PRIEST, G.L. (1996) The government, the market, and the problem of catastrophic loss. *Journal of Risk and Uncertainty*, **12**(2–3), 219–237.
ŠALTYTĖ BENTH, J. and ŠALTYTĖ, L. (2011) Spatial–temporal model for wind speed in lithuania. *Journal of Applied Statistics*, **38**(6), 1151–1168.
SAVU, C. and TREDE, M. (2010) Hierarchies of archimedean copulas. *Quantitative Finance*, **10**(3), 295–304.
SCHNEIDER, K. and ROTH, M. (2013) Growing premium. *Insider Quarterly*. Available at: http://www.insiderquarterly.com/growing-premium
SHI, P. (2014) A copula regression for modeling multivariate loss triangles and quantifying reserving variability. *ASTIN Bulletin: A Journal of the IAA*, **4**(1), 85–102.
SHI, P. and FREES, E.W. (2011) Dependent loss reserving using copulas. *ASTIN Bulletin: A Journal of the IAA*, **41**(2), 449–486.
SIU, T., TONG, H. and YANG, H. (2004) On pricing derivatives under garch models: A dynamic gerber-shiu approach. *North American Actuarial Journal*, **8**, 17–31.
SZÉKELY, G.J. and RIZZO, M.L. (2005) Hierarchical clustering via joint between-within distance: Extending Ward's minimum variance method. *Journal of Classification*, **22**(2), 151–183.
TANKOV, P. (2004) *Financial Modelling with Jump Processes*. Boca Raton: CRC Press.
TURVEY, C.G. (2005) The pricing of degree-day weather options. *Agricultural Finance Review*, **65**(1), 59–85.
TURVEY, C.G., WEERSINK, A. and CHIANG, S.H.C. (2006) Pricing weather insurance with random strike price: The ontario ice-wine harvest. *American Journal of Agriculture Economics*, **88**(1), 696–709.
USDA (2014) *World Agricultural Supply and Demand Estimates Report (WASDE)*. Technical report, Office of the chief economist (OCE), United States Department of Agriculture.
WARD, J.H. (1963) Hierarchical grouping to optimize an objective function. *Journal of the American Statistical Association*, **58**(301), 236–244.
WHELAN, N. (2004) Sampling from archimedean copulas. *Quantitative Finance*, **4**(3), 339–352.
WOODARD, J.D. and GARCIA, P. (2008a) Basis risk and weather hedging effectiveness. *Agricultural Finance Review*, **68**(1), 99–117.
WOODARD, J.D. and GARCIA, P. (2008b) Weather derivatives, spatial aggregation, and systemic risk: Implications for reinsurance hedging. *Journal of Agricultural and Resource Economics*, **33**(1), 34–51.
WOODARD, J.D., SCHNITKEY, G.D., SHERRICK, B.J., LOZANO-GRACIA, N. and ANSELIN, L. (2012) A spatial econometric analysis of loss experience in the U.S. crop insurance program. *Journal of Risk and Insurance*, **79**(1), 261–286.
YANG, J., CHEN, Z., WANG, F. and WANG, R. (2015) Composite bernstein copulas. *ASTIN Bulletin: A Journal of the IAA*, **45**(2), 445–475.
YANG, M. (2011) Volatility feedback and risk premium in Garch models with generalized hyperbolic distributions. *Studies in Nonlinear Dynamics & Econometrics*, **15**(3), 1558–3708.
ZHANG, W., ZHAO, D. and WANG, X. (2013) Agglomerative clustering via maximum incremental path integral. *Pattern Recognition*, **46**(11), 3056–3065.
ZHU, W., WANG, C.-W. and TAN, K.S. (2016) Structure and estimation of Lévy subordinated hierarchical archimedean copulas (LSHAC): Theory and empirical tests. *Journal of Banking & Finance*, **69**, 20–36.
ZHU, W., WANG, C.-W. and TAN, K.S. (2017) Modeling multi-population longevity risk with mortality dependence: A Lévy subordinated hierarchical archimedean copulas (LSHAC) approach. *Journal of Risk and Insurance*, **84**(1), 477–493.

Downloaded from https://www.cambridge.org/core. NTU Library, on 08 Jan 2020 at 04:20:35, subject to the Cambridge Core terms of use, available at https://www.cambridge.org/core/terms. https://doi.org/10.1017/asb.2018.6

WENJUN ZHU (Corresponding author)
Nanyang Business School
Division of Banking & Finance
50 Nanyang Avenue, 639798
Singapore
E-Mail: wjzhu@ntu.edu.sg

KEN SENG TAN
Department of Statistics and Actuarial Science
University of Waterloo
200 University Ave. West
Waterloo, Ontario, Canada
E-Mail: kstan@uwaterloo.ca

LYSA PORTH
Warren Centre for Actuarial Studies and Research
University of Manitoba Asper School of Business
Winnipeg, Manitoba, Canada
E-Mail: lysa.porth@umanitoba.ca

CHOU-WEN WANG
Department of Finance
National Sun Yat-sen University
Kaohsiung, Taiwan
E-Mail: chouwenwang@mail.nsysu.edu.tw

APPENDIX A. STANDARDIZED RESIDUALS OF MARGINAL DISTRIBUTIONS

This appendix display the plots (Figures A1 and A2) and histograms (Figures A3 and A4) of the standard residuals of marginal distributions.

APPENDIX B. THE BEST ESTIMATED LSHAC MODEL

The structure of best estimated LSHAC model based on BIC (the model highlighted in bold with a $\star$ in the parentheses of Table 7) is displayed in Figure A5. The copula model with the corresponding seven Archimedean copula generators are displayed in Equations (B.1)–(B.8).

$$C(\mathbf{AB}, \ldots, \mathbf{QC}) = C_{\psi_0}\big(C_{\psi_{1,1}}\big(C_{\psi_{2,1}}(\mathbf{BC}, C_{\psi_{3,1}}(\mathbf{AB}, \mathbf{SK})), C_{\psi_{2,2}}(\mathbf{MB}, \mathbf{ON})\big), C_{\psi_{1,2}}\big(C_{\psi_{1,2}}(C_{\psi_{2,3}}(\mathbf{NB}, \mathbf{NS}), \mathbf{QC})\big)\big). \quad \text{(B.1)}$$

Downloaded from https://www.cambridge.org/core. NTU Library, on 08 Jan 2020 at 04:20:35, subject to the Cambridge Core terms of use, available at https://www.cambridge.org/core/terms. https://doi.org/10.1017/asb.2018.6

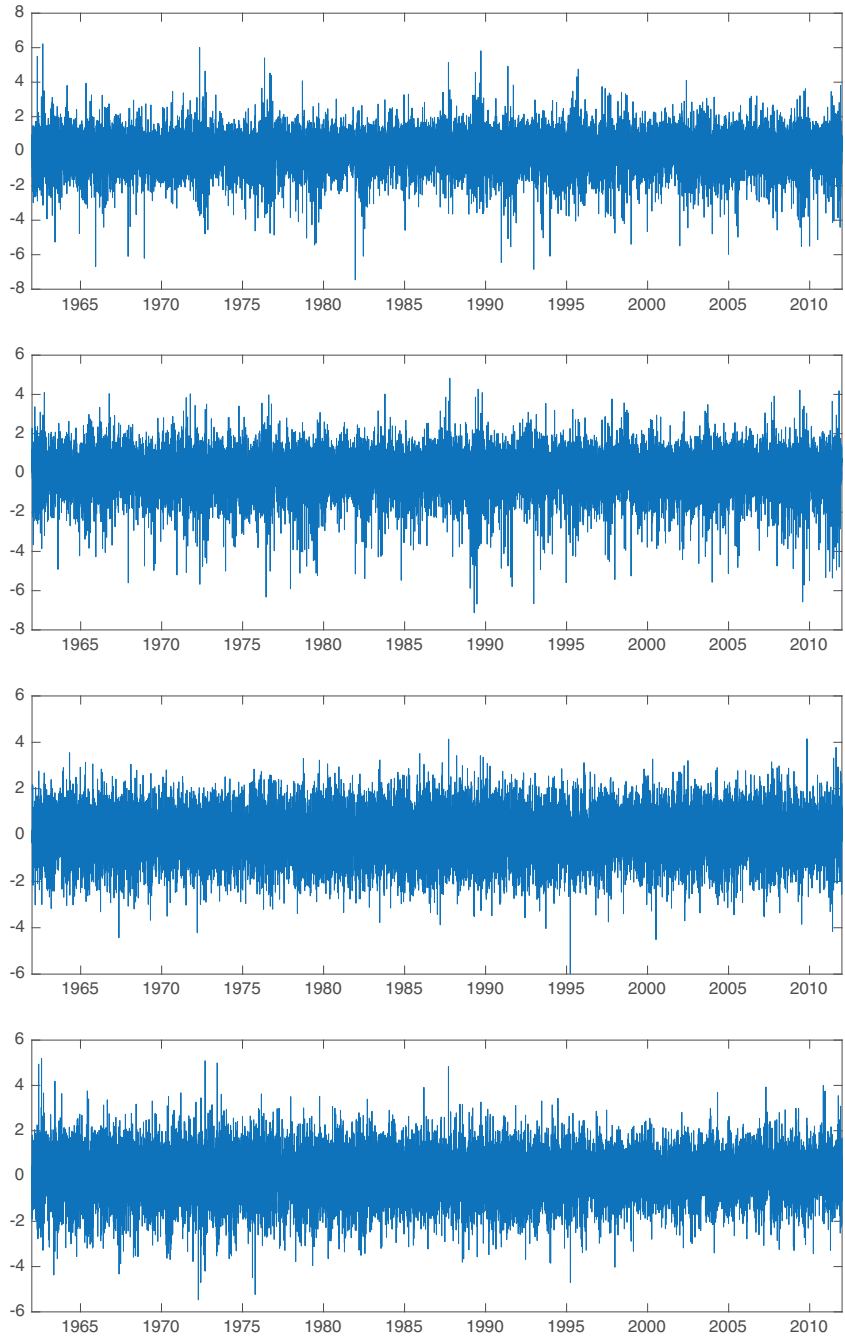


FIGURE A1: Plots of standardized residuals of marginal distributions. Plots are for, from up to down, AB, BC, MB and NB, respectively. (Color online)

Downloaded from https://www.cambridge.org/core. NTU Library, on 08 Jan 2020 at 04:20:35, subject to the Cambridge Core terms of use, available at https://www.cambridge.org/core/terms. https://doi.org/10.1017/asb.2018.6

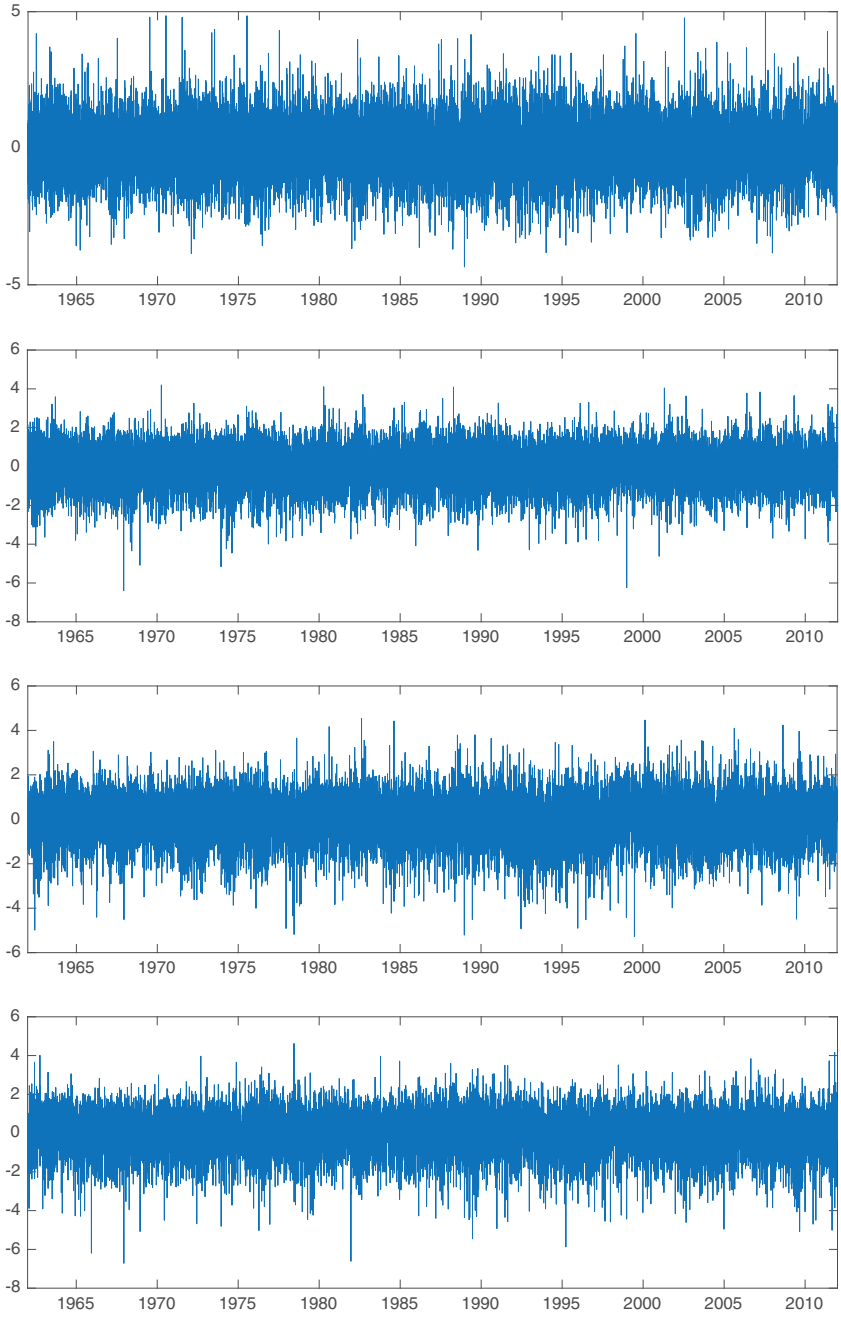


FIGURE A2: Plots of standardized residuals of marginal distributions. Plots are for, from up to down, NS, ON, QC and SK, respectively. (Color online)

Downloaded from https://www.cambridge.org/core. NTU Library, on 08 Jan 2020 at 04:20:35, subject to the Cambridge Core terms of use, available at https://www.cambridge.org/core/terms. https://doi.org/10.1017/asb.2018.6

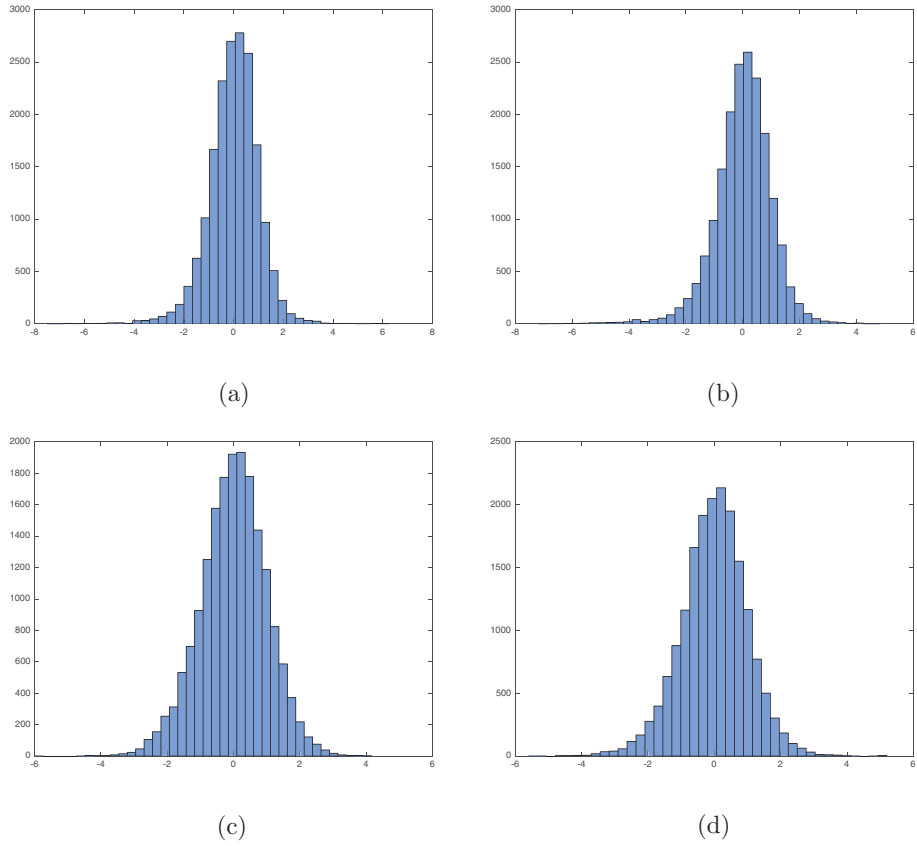


FIGURE A3: Histograms of standardized residuals of marginal distributions. (a) AB, (b) BC, (c) MB, (d) NB. (Color online)

$$\psi_{0,1}(u) = \psi_{\mathrm{CL}}(u) = (1+u)^{-\frac{1}{\theta_0}}, \tag{B.2}$$

$$\psi_{1,1}(u) = \psi_{\mathrm{CL}\circ\mathrm{G}}(u) = (1 + a_{1,1}\log(1+u/b_{1,1}))^{-\frac{1}{\theta_0}}, \tag{B.3}$$

$$\psi_{1,2}(u) = \psi_{\mathrm{CL}\circ\mathrm{St}}(u) = (1+u^{a_{1,2}})^{-\frac{1}{\theta_0}}, \tag{B.4}$$

$$\psi_{2,1}(u) = \psi_{\mathrm{CL}\circ\mathrm{G}\circ\mathrm{St}}(u) = (1 + a_{1,1}\log(1+u^{a_{2,1}}/b_{1,1}))^{-\frac{1}{\theta_0}}, \tag{B.5}$$

$$\psi_{2,2}(u) = \psi_{\mathrm{CL}\circ\mathrm{G}\circ\mathrm{St}}(u) = (1 + a_{1,1}\log(1+u^{a_{2,2}}/b_{1,1}))^{-\frac{1}{\theta_0}}, \tag{B.6}$$

$$\psi_{2,3}(u) = \psi_{\mathrm{CL}\circ\mathrm{St}\circ\mathrm{St}}(u) = (1+u^{a_{1,2}\cdot a_{2,3}})^{-\frac{1}{\theta_0}}, \tag{B.7}$$

$$\psi_{3,1}(u) = \psi_{\mathrm{CL}\circ\mathrm{G}\circ\mathrm{St}\circ\mathrm{St}}(u) = (1 + a_{1,1}\log(1+u^{a_{2,1}\cdot a_{3,1}}/b_{1,1}))^{-\frac{1}{\theta_0}}. \tag{B.8}$$

Downloaded from https://www.cambridge.org/core. NTU Library, on 08 Jan 2020 at 04:20:35, subject to the Cambridge Core terms of use, available at https://www.cambridge.org/core/terms. https://doi.org/10.1017/asb.2018.6

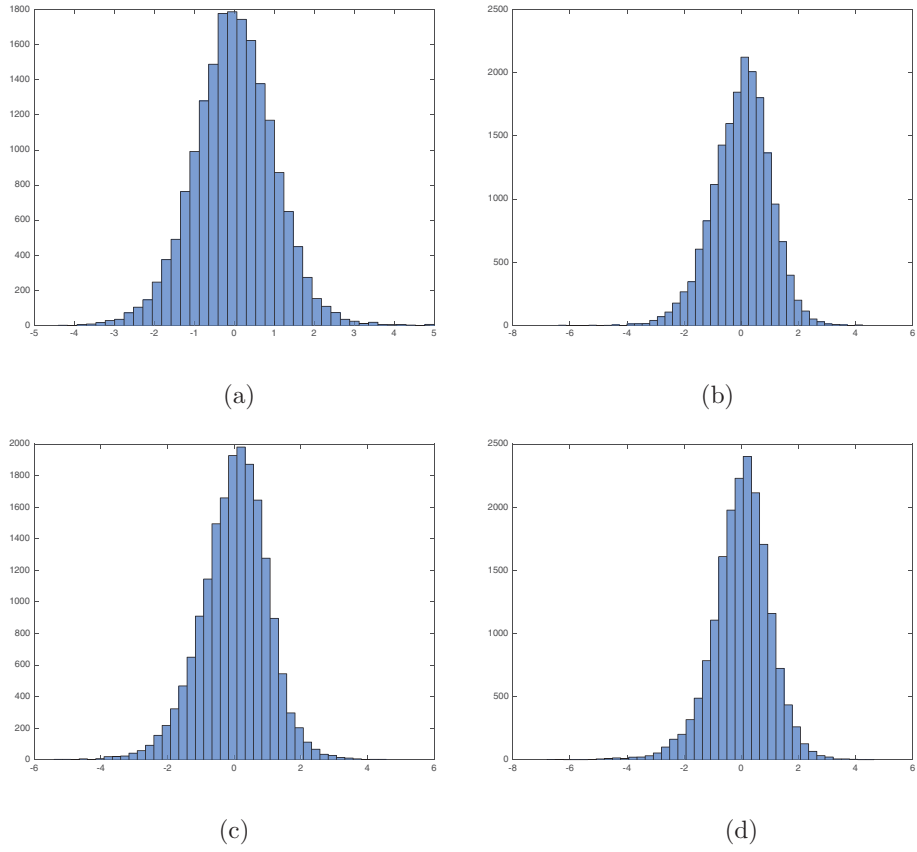


FIGURE A4: Histograms of standardized residuals of marginal distributions. (a) NS, (b) ON, (c) QC, (d) SK. (Color online)

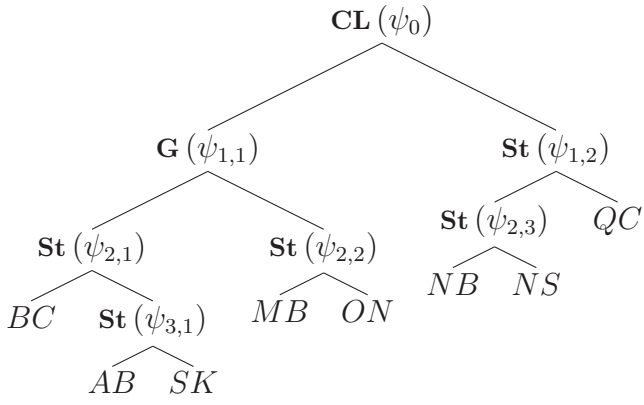


FIGURE A5: The best estimated LSHAC model for the eight Canadian temperature processes.

Downloaded from https://www.cambridge.org/core. NTU Library, on 08 Jan 2020 at 04:20:35, subject to the Cambridge Core terms of use, available at https://www.cambridge.org/core/terms. https://doi.org/10.1017/asb.2018.6